Bull. Chem. Soc. Jpn., 70, 2593—2618 (1997)

Accounts

Preparation of Inorganic–Organic Nanocomposites through Intercalation of Organoammonium Ions into Layered Silicates

Makoto Ogawa* **and Kazuyuki Kuroda†,#**

PRESTO, Japan Science and Technology Corporation and Institute of Earth Science, Waseda University, Nishiwaseda 1-6-1, Shinjuku-ku, Tokyo 169-50

†Department of Applied Chemistry, Waseda University, Ohkubo-3-4-1, Shinjuku-ku, Tokyo 169

(Received April 30, 1997)

Recent developments in the study of the intercalation of organoammonium ions into layered silicates are reviewed. The new developments of the applications of the organoammonium-exchanged layered silicates include the selective adsorption of toxic compounds from water, the immobilization of photo and electroactive species to construct novel photo and electrofunctional materials, and the complexation with organic polymers for the enhancement of the mechanical properties. The conversion of the layered solids to three dimensional nanoporous solids with novel microstructures and adsorptive properties has also been successfully done. The novel controlled properties achieved by the modification with the adsorption of organoammonium ions open new opportunities to tailor the properties of the inorganic-organic nanostructured materials.

Self-organization of molecules into highly ordered architectures has attracted increasing attention from a wide range of scientific interests.[1] The nanostructured materials have an advantage so that the properties of the immobilized species can be discussed on the basis of their defined nanoscopic structures.[2] Their structure-property relationships will provide indispensable information on designing materials with novel chemical, physical, and mechanical properties. Inorganic–organic nanocomposites posses special positions in constructing a supramolecular assembly due to their unique microstructures and the stability.

Intercalation of guest species into inorganic layered solids is a way to construct novel inorganic–organic supramolecular assemblies.[3] Intercalation refers to the act of inserting some extra interval of time into the calendar, such as February 29 in a leap year. In science, it means the reversible insertion of guest species into a layered host materials with maintaining the structural features of the host. (Figure 1 schematically represents intercalation.) The motivation to study intercalation reactions is that the properties of both guest and host can be altered by the reactions. On this basis, intercalation compounds have been studied extensively and a wide variety of host–guest systems with unique structures and the properties have been reported so far.[4] If compared with the inclusion of guest species into zeolites,[5] one of the most important characteristics of intercalation into layered solids is the expandability of their interlayer spaces which make it possible to accommodate a wide variety of guest species. The microscopic structure can be tailored by selecting and designing both the guests and hosts and also by coadsorption. From the X-ray diffraction (XRD) studies, the interlayer distance can be measured and the orientation of the intercalated species can roughly be estimated. Moreover, some materials have been processed into single crystals or oriented films, in which microscopic anisotropy can be converted into macroscopic one.

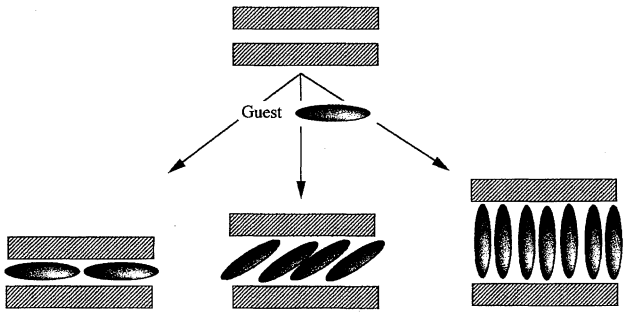

Fig. 1. Schematic representation of intercalation.

The microstructures of the intercalation compounds have been controlled by the host–guest and guest–guest inter-

Kagami Memorial Laboratory for Materials Science and Technology, Waseda University, Nishiwaseda 2-8-26, Shinjuku-ku, Tokyo 169, Japan.

actions. Various layered materials such as graphite, clay minerals, transition metal dichalcogenides, layered double hydroxides, metal phosphates and phosphonates, and transition metal oxides have been known to accommodate guest species in their interlayer spaces to form intercalation compounds.[3] Ion exchange reactions of the interlayer exchangeable cations, adsorption of polar molecules by ion-dipole interaction and hydrogen bonding, acid-base reactions, and charge transfer complex formation have been known to be the driving force for the intercalation.

In this account, the studies on the intercalation of organoammonium ions into the layered solids mainly silicates are summarized. Organoammonium ions are the guest species studied most extensively in the intercalation chemistry partly due to their variation of the molecular structures.[6] The self-organizations of amphiphilic molecules in solutions and on surfaces has widely been investigated to construct novel supramolecular assembly.[7] Stable, ordered surfactant films have many applications, such as controlled permeability membranes, coatings for sensors, and devices for optics and electronics.[8] The assembly of organoammonium ions in the interlayer space of layered silicates can be regarded as a novel state of aggregates confined in a two dimensional nanospace immobilized by the ultra thin inorganic layers. Additionally, the replacement of the interlayer exchangeable cations with organoammonium ions results in the change in the surface properties of host materials. These modified silicates found application to construct novel host–guest systems where hydrophilic silicates do not have an access. The cation exchange with organoammonium ion successfully applied to construct various molecularly designed supramolecular assemblies and the resulting composites have bee employed in a wide variety of scientific and industrial applications.

1. Intercalation of Organoammonium Ions into Layered Silicates

Among possible layered inorganic solids, smectite groups of layered clay minerals have extensively been investigated as host materials, since they possess various attractive features such as the swelling behavior, ion exchange properties, adsorptive properties, large surface area, and so on.[9,10] The cation exchange reactions were conducted by mixing the aqueous suspension of smectites and the solution of organoammonium salts. The products are separated by centrifugation or filtration and washed repeatedly. The cation exchange reactions proceed even in the solid-state where host (smectites) and guest (organoammonium salts) were mixed in the solid-state.[11] Compared with those of smectites, the cation exchange of the interlayer cation of other layered solids usually requires selection of guest species and reaction conditions.

The reaction products have been characterized by a variety of instrumental analyses including X-ray diffraction (XRD), thermal analyses, elemental analyses, electron microscopy, and infrared (IR) and Raman spectroscopies. Recently, infrared spectroscopy has been applied to investigate the states and the orientation of the intercalated alkylammonium ions in the interlayer space of layered silicates.[12,13]

Quantitative ion exchange of the interlayer cations of smectites by alkylammonium ions provides a method for characterization of smectites and determination of their layer charge, which directly correlates the cation exchange capacity.[14] In the interlayer spaces of smectites, the intercalated surfactant cations arranged monolayer and bilayer with their alkyl chains parallel to the silicate sheets and paraffin type layers depending on the size of the intercalated ions and the surface layer charge density as shown in Fig. 2. The arrangements of the intercalated alkylammonium ions depend on the layer charge and the alkyl-chain length. Short-chain

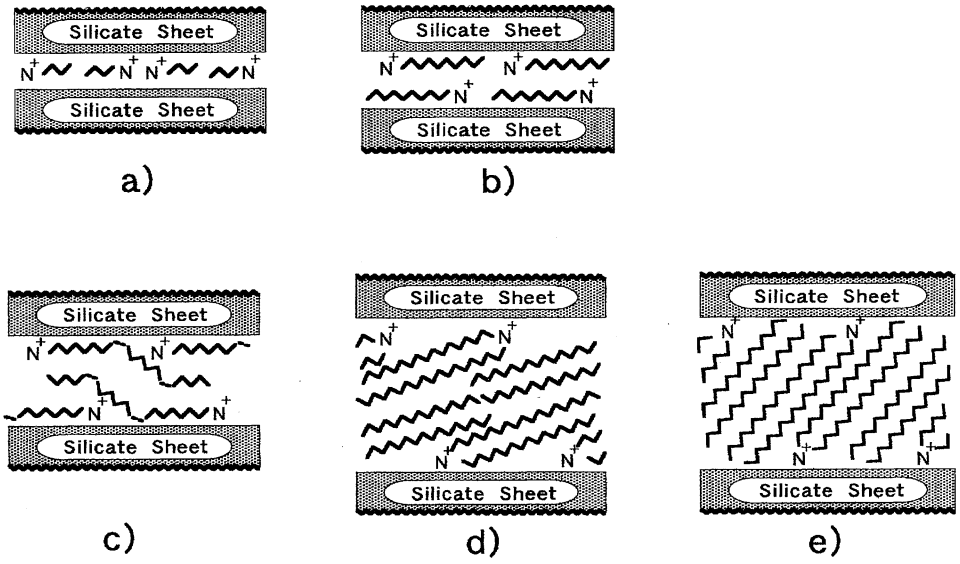

Fig. 2. Schematic drawing for the arrangements of the intercalated alkylammonium ions in the interlayer spaces of smectites. (a) monolayer, (b) bilayer, and (c) pseudo-trimolecular layer. (d) and (e), paraffin type arrangements with mono (d) and bilayers (e).

alkylammonium ions are arranged in monolayer and long chain alkylammonium ions in bilayer with their alkyl chains parallel to the silicate sheets. The monolayer has a basal spacing of ca. 1.4 nm, the bilayer a spacing of ca. 1.8 nm. Since the monolayer rearranges into the bilayer if the area of the flat-lying alkylammonium ions becomes larger than the equivalent area, the monolayer/bilayer transition with increasing the alkyl-chain length can be used as a measure of the surface layer charge density.

Three layers of kinked alkyl chains are observed with highly charged smectites, and referred to *pseudo*-trimolecular layers. The *pseudo*-trimolecular layer system exhibits a basal spacing of ca. 2.2 nm. The alkylammonium ions form paraffin-type aggregates in some layered materials with high layer charge density compared with those of smectites. This type of aggregates can be formed in the interlayer space of smectites with quaternary alkylammonium ions with two or more long chain alkyl groups. The orientation of the alkyl chain in the interlayer spaces depends on the surface layer charge density as shown in Fig. 3.

When the interlayer metal cations of smectites are replaced by cationic surfactants, the hydrophilic surfaces of the smectites are substantially modified to become strongly organophilic.[15] The combination of the hydrophobic nature of the surfactant and the stable layered structures of the silicate sheets led unique physicochemical properties. They have been referred as "organoclay" or "organophilic-clay" and used industrially as rheological controlling agents in paints, greases, and cosmetics.[16] On the other hand, the cation exchange of the interlayer cations with small organic cations such as tetramethylammonium ion, results in the microporous solids where organoammonium ions act as pillar to separate each silicate layers.[17,18] The intercalation of phospholipids into a swelling mica has been reported so far.[19]

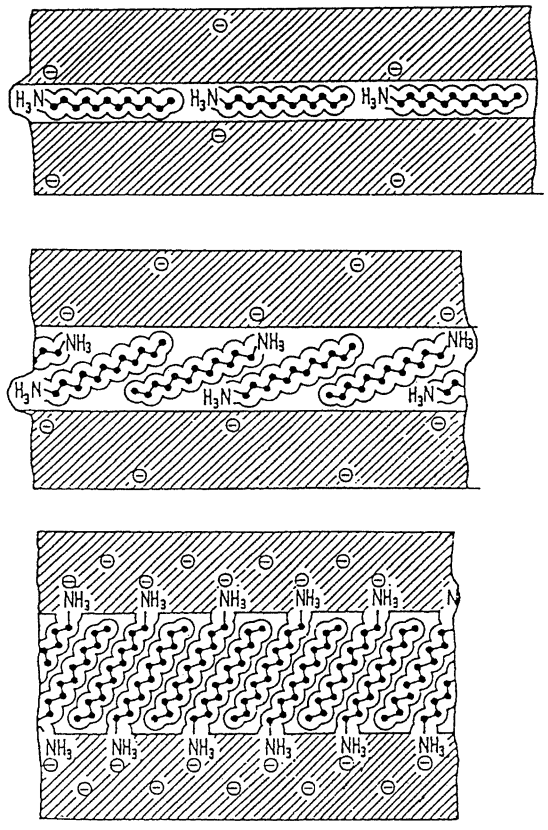

Fig. 3. Schematic structure of alkylammonium ions in the interlayer space of layered materials with different layer charge density.

Long chain organoammonium-modified smectites exhibit swelling behavior in organic solvents, while the tetramethylammonium-smectites swell in water.[20] By simply casting their suspensions in organic solvents or water, they have been processed into thin films with their *ab* plane oriented parallel to the substrate. Self-supporting films are also available.[20,21] These films make it possible to investigate their various physicochemical properties such as photochemical and barrier ones.

The preparation of thin films by means of Langmuir–Blodgett technique from exfoliated platelets of surfactant intercalated silicates is reported recently.[22] The inorganic–organic multilayered films have also been prepared via alternate adsorption of a cationic species and the anionic sheet of an exfoliated layered solid.[23]

Table 1 shows the list of organoammonium ions and their abbreviation used for the modification of layered silicates. Table 2 shows the molecular structures of the photoactive guest species.

2. Immobilization of Guest Species in the Hydrophobic Interlayer Spaces of Organoammonium Exchanged Swelling Layered Silicates

The organoammonium–silicate intercalation compounds can be regarded as novel states of surfactant aggregates immobilized by the ultra thin silicate layers. They have been employed in a wide variety of applications including adsorbents and hosts for polymers and photo and electroactive species. Their microstructures and the modified surface properties play an important role to exhibit unique properties.

2-1. Clay-Polymer Nanocomposites. Preparations of clay-polymer nanocomposites has been investigated widely in order to obtain novel inorganic/organic nanocomposites with enhanced properties such as mechanical ones.[24—26] The preparation methods for the silicate-polymer nanocomposites have been classified into two; one is direct intercalation

Table 1. List of Organammonium Ions Used for the Surface Modification of Layered Silicates Cited in This Account

Organoammonium ions	Abbreviation
Alkylammonium	C_nN^+
Alkyltrimethylammonium ion	$C_n3C_1N^+$
Dialkyldimethylammonium ion	$2C_n2C_1N^+$
Tetramethylammonium ion	TMA
Tetrapropylammonium ion	TPA
Tetrapentylammonium ion	TPeA
Trimethylphenylammonium ion	TMPA
Alkylpyridinium ion	C_nPy^+

Table 2. The Molecular Structures of the Guest Species

Spiropyran	SP	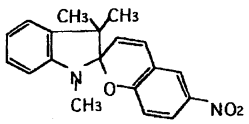
Azobenzene		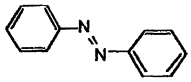
Anthracene		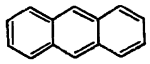
Pyrene		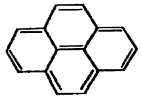
Quinizarin	DAQ	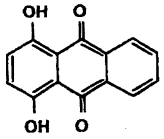
p-Nitroaniline		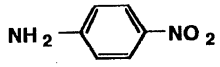
Methylviologen	MV^{2+}	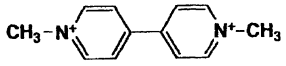

of polymer into the layered silicates and the other is polymerization of the intercalated monomers in the interlayer spaces.

Organoammonium exchanged montmorillonites have been used as precursor for the introduction of acrylonitrile and the subsequent polymerization in the adsorbed states led the novel clay–poly(acrylonitrile) composites.[27] The resulting clay polymer composites have been converted to non-oxides ceramics by a carbothermal reduction in which the adsorbed poly(acrylonitrile) acted as carbon sources. The adsorption of acrylonitrile on inorganic ion montmorillonites and the polymerization in the interlayer spaces have been investigated so far.[28] The notable feature of the organoammonium–montmorillonite–poly(acrylonitrile) intercalation compounds is the large amount of the poly(acrylonitrile), which made it possible to reduce oxide lattice completely. The ion–dipole interactions between the interlayer exchangeable cations and the acrylonitrile molecules are the driving force for the intercalation into inorganic ion montmorillonites, so that the amounts of the adsorbed acrylonitrile molecules have been limited compared to those achieved for the organoammonium–clay–acrylonitrile systems.

This synthetic approach has been applied to the carbothermal reduction of magadiite[29] and hydrotalcite.[30] Magadiite is a layered silicate with the ideal formula of $Na_2Si_{14}O_{29}\cdot nH_2O$, where the interlayer sodium ions can be exchanged. Hydrotalcite is a layered metal double hydroxide composed of a layered magnesium hydroxide in which aluminum ions substitute a portion of magnesium to cause net positive charge of the layer. To compensate the positive charge, anions such as carbonate occupy the interlayer space and they can be replaced with inorganic and organic anions. The dodecyltrimethylammonium–magadiite and the hydrotalcite–dodecyl sulfate intercalation compounds have been prepared and used to accommodate poly(acrylonitrile) molecules. The formations of silicon nitride and carbide from magadiite and aluminum nitride from hydrotalcite have been observed by the carbothermal reduction.

Since the discovery of the improved mechanical properties of engineering polymers by reinforcing the exfoliated clay platelets, the researches on the clay–polymer interactions have attracted new interests.[31–38] Fukushima and his co-workers discovered the several clay–polymer hybrids including systems based on the dispersion of alkylammonium-exchange montmorillonites in nylon-6, epoxides, and polyimides.[31] The ion exchange of the organoammonium ions makes it possible to accommodate large amount of organic polymers in the interlayer space or in turn the dispersion of clay platelets in polymer networks. In these systems, it is more appropriate to consider that the clay platelets have been guests doped in polymer hosts. The properties of clay–polymer hybrids are often far superior to those of pristine polymers and conventional composites. The addition of 4.7 wt% montmorillonite to nylon-6 increased the tensile strength and modulus. The thermal and rheological properties of the nylon were improved significantly by the reinforcement of montmorillonites.

These composites have been prepared by the intercalation of monomer into the alkylammonium exchanged montmorillonites and subsequent heat treatment. Although the microstructure of the heat treated products are unclear, the composites exhibited improved barrier properties. The interactions occurring at the polymer–organoclay interface are very complex. The polymer may bind (adsorb) directly to the chemically inert network of siloxane oxygen atoms on the basal surface of the silicate layers. In addition, the alkylammonium chains may "dissolve" to different degrees into the polymer matrix. These interfacial interactions are schematically represented by Shi et al. (Fig. 4).[36] The possible catalytic effect of the interlayer onium ions on the intragallery polymerization has also been proposed.[36]

An alternative synthetic approach has been reported.[37,38] $C_{18}N^+$- and $C_{12}N^+$-fluorohectorite and polymers (polysty-

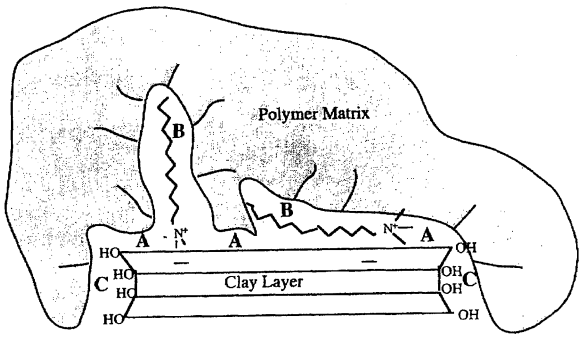

Fig. 4. Schematic drawing for the interfacial interactions of polymer–organoclay composites. Reprinted from Ref. 36. Copyright 1996 American Chemical Society.

rene and poly(3-bromostyrene)) were mechanically mixed and formed into a pellet using a hydraulic pressure. The pellets were subsequently annealed in vacuum at temperature higher than the glass transition temperature of polymers. The X-ray diffraction studies on the clay–polymer composite systems showed the expansion of the interlayer space and the dispersion of silicate plates in polymers has been revealed by the TEM observations.

The presence of organoammonium ions in the interlayer spaces is necessary to accommodate organic polymers in some cases. In connection with these organoclay–polymer systems described above, the adsorption of enzymes into layered silicates is a notable example.[39,40] The adsorption of enzyme on smectites is ordinarily pH dependent, while the enzyme may be strongly bound by alkylammonium–clays by hydrophobic interactions. Such interactions may involve hydrophobic portions of the enzyme interacting with the hydrophobic alkyl group on the mineral surface. Enzymes such as urease and glucose oxidase have been immobilized on the organically modified smectites.

2-2. Adsorbents for Poorly Water Soluble Organic Species. The adsorptive properties of the organoammonium-exchanged smectites have long been recognized.[17,18] When the interlayer exchangeable cations are inorganic ions such as Na and Ca, the cations are strongly hydrated in the presence of water and the ion–dipole interactions prevent the adsorption of poorly water soluble organic nonionic species such as aromatic hydrocarbons that move from contaminated sites into ground waters. The surface properties can be altered by cation exchange with organoammonium ions to become highly effective in removing such compounds from water.[41]

Organoammonium-smectites have been prepared by the conventional ion exchange method and used as adsorbents. Excess organic salts may be adsorbed by the clay in large excess of the cation exchange capacity, excess organic salts were not added for the ion exchange. Because these organic cations are strongly preferred by the exchange sites over the Na ions, most of the organic cations was taken up from solution. The amounts of the adsorbed organoammonium cations are just around the cation exchange capacity of the clays.

Adsorption isotherms were obtained by the technique which consists of adding a solution containing a known amount of the organic compound, shaking it for 12—24 h, centrifuging, and testing the remaining solution for the amount of organic compound that was not adsorbed. The ultraviolet spectroscopy has been utilized to determine the amounts of organic compounds.

The adsorption isotherms of phenol (D), 3-chlorophenol (C), 3,5-dichlorophenol (B), and 3,4,5-trichlorophenol (A) from water onto $C_{16}3C_1N^+$-smectite are shown in Fig. 5.[41a] The isotherm showed significant difference for the various phenols. As the number of chlorine atoms or the benzene ring was increased, the greater amount was adsorbed. Similar isotherms were obtained for the adsorption of phenols on $C_{16}Py^+$-smectite. These data indicate that as chlorine atoms

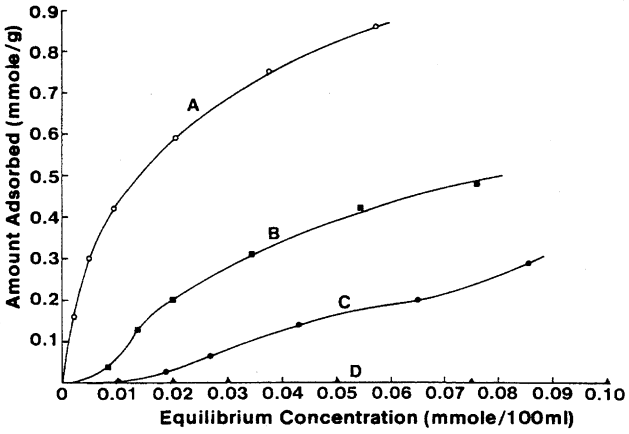

Fig. 5. The adsorption isotherms (20 °C) of phenols on the $C_{16}3C_1N^+$–smectite. A = 3,4,5-trichlorophenol; B = 3,5-dichlorophenol; C = 3-chlorophenol; D = phenol. Reprinted from Ref. 41a. Copy right 1986 The Clay Minerals Society.

were added to the phenol structure, adsorbent–adsorbate interaction with $C_{16}3C_1N^+$ and $C_{16}Py^+$ increased.

However, the adsorption isotherms of the phenols on the trimethylphenylammonium (TMPA)-smectites are quite different (Fig. 6). More amounts of phenol were adsorbed than any of the chlorinated analogs. The phenol isotherm was a typical type V isotherm with indicates weak adsorbate–adsorbent interaction. The adsorption of phenol and chlorophenols into the organoammonium-smectites revealed that the intercalation compounds with long chain alkyl groups were the most hydrophobic and adsorbed phenols from water in proportion to their hydrophobicity. The adsorption of pentachlorophenol showed similar tendency. The hydrophobic-clays ($2C_{16}2C_1N^+$- and $C_{16}3C_1N^+$-clays) adsorb greater amounts of pentachlorophenol than the organoammonium–clays containing small organic cations.

The adsorption of phenols from hexane into organoammonium-smectites exhibits different tendency. Whereas 3,4,5-trichlorophenol was strongly adsorbed on $C_{16}3C_1N^+$-smectites from water, phenol was not adsorbed at all. On the other

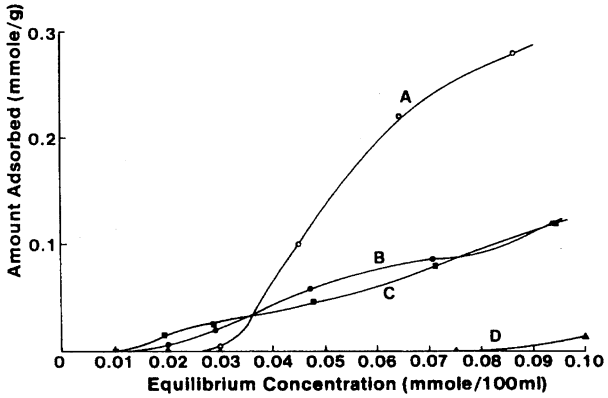

Fig. 6. The adsorption isotherms (20 °C) of phenols on the trimethylphenylammonium-smectite. A = phenol; B = 3-chlorophenol; C = 3,4,5-trichlorophenol; D = 3,5-dichlorophenol. Reprinted from Ref. 41a. Copyright 1986 The Clay Minerals Society.

hand, the two species were adsorbed to similar degrees. This difference has been ascribed to the relative importance of both adsorbate–solvent and adsorbate–surface interactions on the partitioning of adsorbate molecules between solvent and surface. In water, phenol interacted strongly with water and was not attracted sufficiently to the hydrophobic surfaces $C_{16}3C_1N^+$- and $C_{16}Py^+$-smectites to cause a significant adsorption. Phenol had a much less interactions with hexane, and the adsorbent–adsorbate interactions were strong enough to result in considerable adsorption.

The different adsorption was observed for isomers of the same compounds (3,4,5-trichlorophenol and 2,4,6-trichlorophenol). This suggests that the precise molecular sieving effect can be obtained using organoammonium-smectites as adsorbents, although the details in the reaction mechanisms are unclear at present.

The adsorption of benzene, perchloroethene, and 1,2,-dichlorobenzene into $C_{16}3C_1N^+$-clays from water has been investigated.[41b] These organic species are common organic groundwater pollutants. The uptake of benzene, perchloroethene, and 1,2,-dichlorobenzene increased dramatically after the treatment of clays with $C_{16}3C_1N^+$. The clay type affects the adsorption characteristics. The $C_{16}3C_1N^+$–clays with greater amount of $C_{16}3C_1N^+$ showed increased nonionic organic sorption. Greater sorption of alkylbenzens (ethyl-, propyl, and butyl-benzenes) by the high layer charge $C_{16}3C_1N^+$–clays has been observed, suggesting the capability of the large basal spacings to accommodate larger solute molecules.[41d]

The adsorption behavior on the $C_{16}3C_1N^+$-montmorillonite has recently been investigated by means of Raman spectroscopy.[42] Since water is an extremely weak Raman scatter, the use of a Raman band associated with the interlayer organoammonium ions as an internal standard gave adsorption isotherms. The adsorption of iodide, caesium, and strontium on the $C_{16}Py^+$-vermiculite has also been investigated.[43]

Srinivasan and Fogler described the synthesis of organically modified pillared clays for use in wastewater treatment.[44] The adsorption of benzo[*a*]pyrene and chlorophenols on organically modified hydroxyaluminium–montmorillonite has been investigated. These pillared and organically modified montmorillonite exhibited greater ability to accommodate such compounds from water than organically modified-montmorillonites.

Adsorption of organic vapor in air also requires a wide range of adsorbents.[45,46] Yan and Bein have investigated the adsorption isotherm of organic vapors and nitrogen by means of quartz crystal microbalance (QCM).[45a] The experimental set-up for the measurements is shown in Fig. 7. Organoammonium-hectorites were coated on the gold electrodes of the QCM by dipping the crystal in their suspensions. Water, acetonitrile/water or chloroform was used as solvents depending on the dispersion properties of the organoammonium-hectorites. TMA-, tetrapropylammonium (TPA)-, tetrapentylammonium (TPeA)-, $C_{18}3C_1N^+$-, $2C_{18}N^+$-, and methyltrioctadecylammonium ($3C_{18}C_1N^+$)-forms have been investigated. They concluded that the organoammonium-

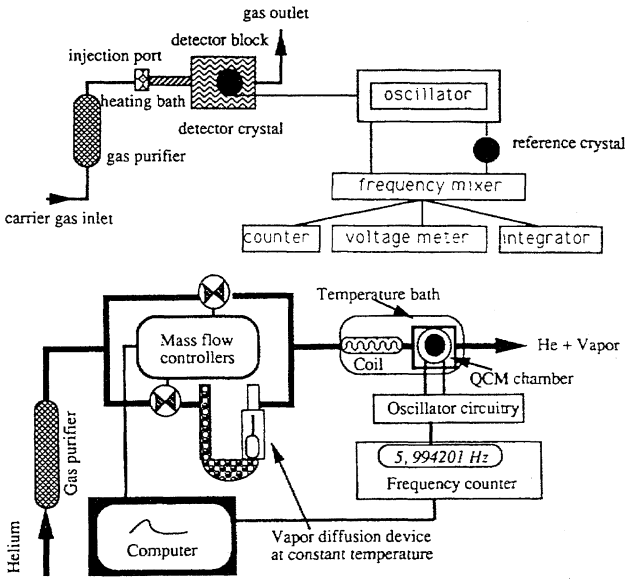

Fig. 7. (top) Schematic diagram of the apparatus for transient sorption of vapor pulses by QCM. (bottom) Schematic diagram of the apparatus for vapor sorption isotherms. Reprinted from Ref. 45b. Copyright 1992 American Chemical Society.

smectites can be possible candidates for selective chemical sensors. The interplay of size exclusion and partitioning in the organic phases results unique selectivities.

Organic modification with small organic cations such as TMA results in the adsorption characteristic different from that on the long chain organoammonium-exchanged forms.[47] The adsorption of benzene, toluene, and xylene on TMA-smectites with different layer charge density as vapors by the dry clay and as solutes from water has been investigated.[48] In the adsorption of organic vapors, the closer packing of the TMA ions in the high-charge TMA-smectite, resulted in a higher degree of shape selective adsorption. In the presence of water, the adsorption capacities for aromatic molecules were significantly reduced. The lower sorption capacity was accompanied by increased shape selectivity. The reduction in uptake and increased selectivity was much more pronounced for the water saturated, high charge TMA-smectite than for the low charge TMA-smectite. Hydration of the TMA ions and/or the siloxane surfaces apparently reduces the accessibility of the aromatic molecules to interlamellar regions. The low charge TMA-smectite was highly effective adsorbent for removing benzene from water and may be useful for purifying benzene-contaminated water.

The adsorption of aromatic and chlorinated hydrocarbons on tetramethylphosphonium-smectite has been investigated and the results indicated that the tetramethylphosphonium-smectites is a better adsorbent than the TMA-smectites in the presence of water due to lower degree of hydration of the tetramethylphosphonium cation than that of the TMA cation.[49] The adsorption of aromatic hydrocarbon on the trimethylphenylammonium (TMPA)-smectites has been investigated.[50] Smectites with a range in layer charge density have been used to control the microstructures as schemati-

cally shown in Fig. 8. The adsorption increased as layer charge decreased, suggesting the strong adsorption of hydrophobicity of the siloxane surfaces in smectites.

The infrared study of water sorption on TMA- and TMPA–montmorillonite revealed that water preferentially hydrates the TMA and TMPA, not the siloxane surface of montmorillonite.[51] The orientation of TMPA cations in the interlayer space of montmorillonite has recently been investigated by means of infrared dichroism. The orientation affects the adsorbate accessible siloxane surface area and determines whether the TMPA phenyl ring can interact with other aromatic adsorbates.

2-3. Surfactant Intercalated Clay Films for Electrochemical Reactions. Rusling and his co-workers studies the electrochemical reduction of trichloroacetic acid using dialkyldimethylammonium ($2C_n2C_1N^+$)-intercalated bentonites with dissolved cobalt and iron phthalocyanines in the hydrophobic interlayer spaces.[52] Catalytic current vs. temperature plots for the catalytic reduction showed linear branches with intersection points at 5 and 54 °C for 2 $C_{12}2C_1N^+$ and $2C_{18}2C_1N^+$-forms, respectively. The temperature was thought to reflect the gel-to-liquid crystal phase transition of the interlayer $2C_n2C_1N^+$ aggregates.[52a] The gel-to-liquid crystal phase transition has been observed for the study in the permeability of $2C_n2C_1N^+$–montmorillonite films[53] and has also been examined by means of the fluorescence of pyrene[54] and the photochromic reactions of a spiropyrane.[55]

It has been reported that cobalt(II) phthalocyanine was a much better catalyst than the corresponding iron(II) complex.[52] Spectroscopic, X-ray, and electron microscopic studies suggested that iron(II) phthalocyanine is present in oxidized form in the clay–surfactant films.[52b] The state of the iron(II) phthalocyanine in the films was thought to be responsible for the lower catalytic activity. The scanning electron micrograph and X-ray diffraction patterns of the composite films showed that the films are composed of the phthalocyanine complex crystals and surfactant bilayer intercalated clays. It is supposed that a part of phthalocyanine complexes adsorbed in the surfactant bilayers are catalytically active and are responsible to the observed temperature dependence of the catalytic currents.

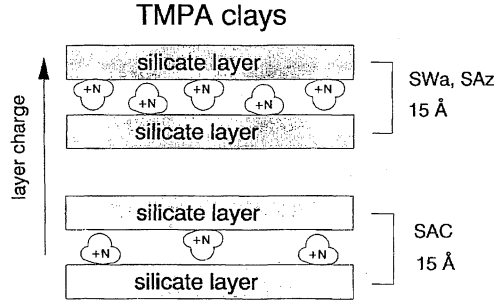

Fig. 8. Schematic drawing for the microstructures of the TMPA–smectites. SAC, SAZ, and SWa denote a Wyoming montmorillonite, a Arizona montmorillonite, and a Washington nontronite, respectively. Reprinted from Ref. 50. Copyright 1991 The Clay Mineral Society.

The electrochemical behavior of a clay modified electrode when the cationic surfactant was present in the electrolytic solutions has been reported.[56] $C_{16}3C_1N^+$ ions were adsorbed readily to a positive double layer on the surface of the clay particles. The formation of cationic surfactant bilayer conferred anion exchange properties to a surfactant adsorbed clay modified electrode. A hydrophobic compounds was also concentrated at the electrodes.

2-4. Photoprocesses of Poorly Water Soluble Photoactive Species. Intercalation compounds have been characterized by a wide variety of instrumental analyses. Spectroscopic properties of the adsorbed species, which are very sensitive to the environment, have given insight to the microscopic structures of the host–guest systems, to which conventional instrumental analysis does not have an access. By utilizing photoprocesses of adsorbed photoactive species, one can obtain microscopic information such as the distribution and mobility of the guest species.[57] Besides the scientific importance, these studies are of practical significance because they provide indispensable information on designing photofunctional materials using layered solids. Photofunctions such as photochromism, photoluminescence, photochemical hole burning, and nonlinear optical properties of the intercalation compounds have been investigated so far.[4a]

Photochromism, dealing with photochemical reactions which are thermally or photochemically reversible, has received considerable attention because of its actual and potential applications and for its paramount importance in biological phenomena.[58] Studies on photochromic reaction behaviors and their controls in solid media have significance for practical applications such as in optical recording as well as in probing host–guest systems. On this basis, photochromisms of fulgides,[59] spiropyrans,[55,60,61] azobenzenes,[62—66] and methylviologen,[67] intercalated in the interlayer space of smectites have been reported. One may expect the change in the physicochemical properties of the intercalation compounds induced by the photochromic reactions. The long chain organoammonium-modified silicates have been used for the introduction of azobenzene[62—64] and spiropyrans[55,60,61]. The role of the surfactant is not only for producing hydrophobic interlayer spaces, but for controlling the states of the adsorbed dyes.

Seki and Ichimura have investigated the thermal isomerization kinetics of photoinduced merocyanine (MC) to spiropyran (SP) in solid films having multibilayer structures, which consist of ion complexes between ammonium bilayers forming amphiphiles ($2C_{18}2C_1N^+$) and polyanions (montmorillonite and poly(styrene sulfonate), abbreviated as PSS).[55] The photochromic reaction of spiropyran is shown in Scheme 1. 1,3,3-Trimethyl-6′-nitrospiro[2*H*-1-benzopyran-2,2′-indoline] (SP) was incorporated into thin film of the polyion complexes, which were prepared by casting the chloroform solution or suspension of the polyion complexes.

X-Ray diffraction studies showed that the cast films were composed of a multilamellar bilayer structure whose membrane plane was preferentially oriented parallel to the film

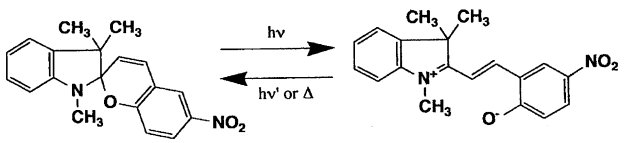

Scheme 1. Isomerization of spiropyran to merocyanine.

surface. Endothermic peaks were observed in the DSC (differential scanning calorimetry) curves of the films; the observed phase transition temperature was 54.5 and 48.5 °C for the $2C_{18}2C_1N^+$–montmorillonite and $2C_{18}2C_1N^+$–PSS films, respectively. The results of DSC and X-ray diffraction indicated that the $2C_{18}2C_1N^+$-montmorillonite film had a more ordered structure than $2C_{18}2C_1N^+$–PSS film. Since annealing the film at 60—70 °C at a relative humidity of ca. 100% for a few hours resulted in the well-structured $2C_{18}2C_1N^+$–PSS film, the photochromic behavior was investigated for the annealed films. The difference in the film structure influences the kinetic properties of the thermal decaying of MC embedded in the films.

The incorporated SP exhibited photochromism in both of the immobilized bilayer complexes with montmorillonite and PSS. Kinetic measurements of the thermal isomerization (decoloration) were carried out for the annealed film. The decoloration reaction rate (Table 3) is dependent on the mobility of the surroundings and, in polymer matrices, is influenced by the glass transition. It was found that the reaction rates abruptly increased near the gel to liquid-crystal phase-transition temperature (54 °C) of the immobilized bilayer due to increased matrix mobility in this system. Figure 9 shows the Arrhenius plots for decaying rates of photoinduced merocyanine (abbreviated as PMC) embedded in annealed $2C_{18}2C_1N^+$–montmorillonite and $2C_{18}2C_1N^+$–PSS films. The film prepared with montmorillonite gives more homogeneous reaction environments for the chromophore than those with the linear polymer (PSS). This leads to drastic changes in this reaction rate at the crystal to liquid-crystal phase transition of the bilayer, showing the effect of the phase transition of immobilized bilayers to be more pronounced

Table 3. Kinetic Data of Thermal Decoloration of PMC in $2C_{18}2C_1N^+$–PSS (a) and $2C_{18}2C_1N^+$–Montmorillonite (b) Films Reprinted from Ref. 55. Copyright 1990 American Chemical Society.

Film	k at 30 °C/s^{-1}		k_{film}/k_{sol}	Factor of rate jump at T_c [a]	E_a/kJ mol^{-1}	
	k_{film}	k_{sol}			Below T_c	Above T_c
$2C_{18}N^+2C_1$–PSS[b]	1.6×10^{-2} (fast)	2.2×10^{-2} [c]	0.72	2.6		
	7.6×10^{-4} (slow)		0.035	4.9	14.2	38.5
$2C_{18}N^+2C_1$–Mont[b]	6.8×10^{-4} (fast)	7.9×10^{-3} [d]	0.086	2.0		
	4.8×10^{-5} (slow)		0.0061	14	53.5	89.9

a) For the evaluation of the rate jump at T_c, see the text. b) Annealed films. c) In water–1,4-dioxane (3/97), λ_{max} = 565 nm. d) In water–1,4-dioxane (7/93), λ_{max} = 555 nm.

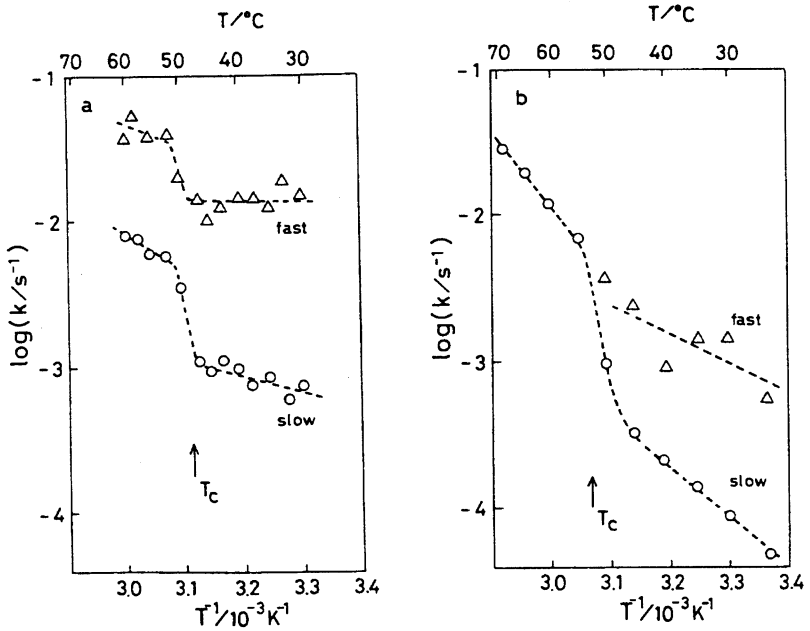

Fig. 9. Arrhenius plots for decaying rates of PMC embedded in annealed $2C_{18}2C_1N^+$–PSS(a) and $2C_{18}2C_1N^+$–montmorillonite (b) films. Slow (○) and first (△) componets. Arrows indicate the phase transition temperature obtained in DSC measurements. Reprinted from Ref. 55. Copyright 1990 American Chemical Society.

than that of the glass transition of amorphous polymer matrices.

The gel-to-liquid crystal phase transition has been investigated by means of luminescence probes 1,3-di(1-pyrenyl)propane and pyrene.[54] Aromatic hydrocarbons such as pyrene have been employed as a luminescence probe of polarity and microviscosity in a variety of organized assemblies. Pyrene is a good excimer forming probe due to the long life time of fluorescence and formation of excited state dimers (excimers) at low concentration. The ratio of excimer to monomer fluorescence intensity obtained from emission spectra is often utilized as a measure of pyrene mobility and proximity. The vibronic fine structure of pyrene monomer is sensitive to surrounding polarity.[69] Pyrene and anthracene themselves are poorly adsorbed on the hydrophilic surface of smectites but are readily adsorbed by organoammonium-intercalated clays. 1,3-Di(1-pyrenyl)propane can be a better probe than pyrene for microviscosity studies. Because it has two pyrene moieties in a molecule, 1,3-di(1-pyrenyl)propane forms intramolecular excimers at extremely low concentrations.

$2C_{18}2C_1N^+$- and $2C_{12}2C_1N^+$–bentonite films containing pyrene or 1,3-di(1-pyrenyl)propane have been prepared by casting their suspensions in chloroform on In-doped SnO_2 electrodes and luminescence has been examined at a temperature range from 0 to 75 °C.

The relative intensity of excimer peak increased gradually with increasing temperature as shown in Fig. 10, suggesting a lower viscosity at temperature above the phase transition. The discontinuities have been observed for the $2C_{12}2C_1N^+$- and $2C_{18}2C_1N^+$–clay films. The phase transition temperature has been estimated from the data to be 7.4 and 53 °C for the $2C_{12}2C_1N^+$- and $2C_{18}2C_1N^+$–clay films. These temperatures are in agreement with those measured by DSC. In the gel state, surfactant hydrocarbon chains are all in the *trans* conformation, causing rigidity. In the liquid crystalline states, the surfactant alkyl chains contain a fraction of *gauche* conformation of C–C bonds to produce kinks, which produces more fluidity. The enhanced excimer peak of 1,3-di(1-pyrenyl)propane reflects the increase in the mobility of the alkyl chains. These results are consistent with the increased diffusion rates of solutes in the $2C_n2C_1N^+$–clay films above the phase transition temperature. The phase transitions of the $2C_n2C_1N^+$–silicates have also been investigated by means of temperature dependence of pyrene fluorescence as well as photochromism of azobenzene.

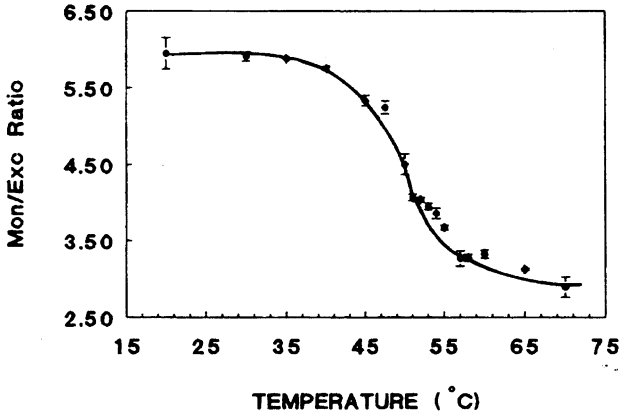

Fig. 10. Ratios of monomer/excimer peaks from emission spectrum of 1,3-di(1-pyrenyl)propane in $2C_{18}2C_1N^+$–clay film. Reprinted from Ref. 54. Copyright 1995 American Chemical Society.

An important aspect of the $2C_n2C_1N^+$–clay films is the change in the states of guest species by soaking in water. The probes are initially solubilized in a polar region close to the head groups of the surfactant. This region is thought to be relatively rigid, and this might explain the observed large microviscosities. On soaking in water, the probe microenvironment slowly becomes less polar and much less viscous.

Intercalation of pyrene, anthracene, and azobenzenes into the long chain quaternary alkylammonium-smectites was successfully achieved by solid-solid reactions which we have developed.[69–71] The mixture of a host material and a guest species was ground with a mortar and a pestle at room temperature. The hydrophobic interactions between the guest species and organoammonium ions are thought to be the driving force for the intercalation. By the solid-state reaction between the $C_{18}3C_1N^+$–montmorillonite and pyrene, a new d(001) diffraction peak with the basal spacing of ca. 3.7 nm appeared and the intensity of the d(001) diffraction peak due to the unreacted $C_{18}3C_1N^+$-montmorillonite decreased as shown in Fig. 11a. The change in the XRD pattern of the $2C_{18}2C_1N^+$–montmorillonite by the reaction with pyrene is different. The basal spacings increased gradually up to 3.8 nm depending on the relative amount of the added anthracene (Fig. 11b). While the basal spacing of the $C_{18}3C_1N^+$–montmorillonite–pyrene intercalation compound was 3.6 nm, the basal spacings of the $2C_{18}2C_1N^+$–montmorillonite–pyrene intercalation compounds varied gradually from 3.0 to 3.9 nm depending on the amounts of the added pyrene. The arene molecules are solubilized at extremely high concentrations in the two dimensional interlayer spaces of the alkylammonium–montmorillonites while retaining the ordered structure which was evidenced by the X-ray diffraction studies.

Fluorescence spectra of the intercalated arenes as well as the X-ray diffraction patterns show that two different types of adsorption occurred. The arenes in the $C_{18}3C_1N^+$–montmorillonite are aggregated and those in the $2C_{18}2C_1N^+$–montmorillonite are rather dispersed between the alkyl-chains in the interlayer spaces. This difference in the adsorption state is due to the arrangements of the interlayer alkylammonium ions. If the cations are arranged parallel to the silicate sheets, adsorbed arenes tend to aggregate. The arene molecules intercalated into the alkylammonium-smectites with paraffin type arrangement of the interlayer organoammonium ions tend to solubilize the hydrocarbons molecularly.

In the fluorescence spectra of the pyrene intercalated compounds, monomer fluorescence with vibrational structure was observed around 400 nm together with the broad peak due to excimer emission (500 nm). The ratio of monomer to excimer for the $2C_{18}2C_1N^+$–montmorillonite system is three

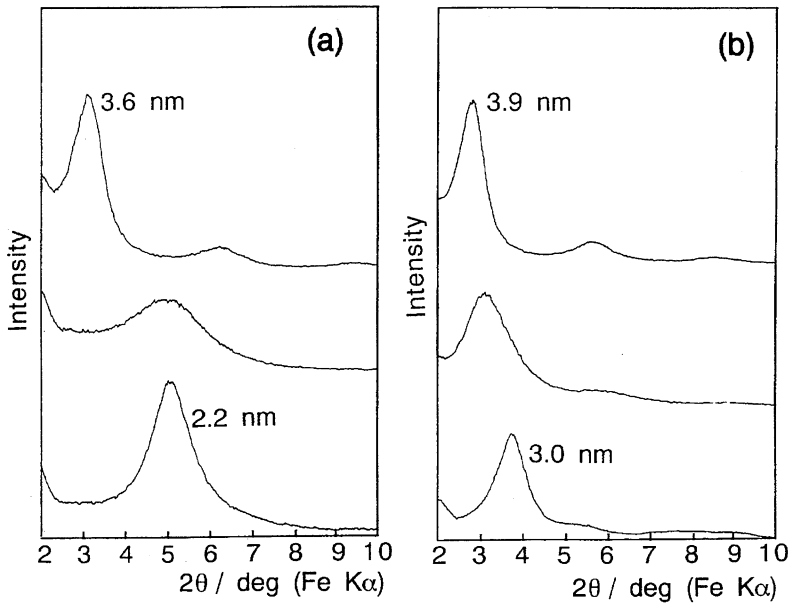

Fig. 11. The change in the X-ray diffraction patterns of the $C_{18}3C_1N^+$– (a) and $2C_{18}2C_1N^+$–montmorillonites (b) by the solid-state reactions with pyrene. Reprinted from Ref. 70. Copyright 1993 American Chemical Society.

times higher than that for the $C_{18}3C_1N^+$-system, suggesting that the adsorbed pyrene molecules are isolated in the interlayer space of the $2C_{18}2C_1N^+$–montmorillonite compared with those doped in the $C_{18}3C_1N^+$–montmorillonite.

Similar results have been observed when fluorotetrasilicic mica (TSM) was used as the host material.[71] The basal spacings and the amounts of the adsorbed organoammonium cations of the $2C_{18}2C_1N^+$– and $C_{18}3C_1N^+$–TSMs were similar to those of the corresponding organoammonium–montmorillonites, suggesting similar arrangements of the intercalated quaternary ammonium ions in the interlayer spaces. The changes in the X-ray diffraction patterns for the reactions of the two organoammonium–TSMs with anthracene or pyrene were also similar to those observed for the montmorillonite systems.

The spectroscopic properties of the intercalated pyrene molecules showed a similar difference. The luminescence spectra of the $2C_{18}2C_1N^+$- and $C_{18}3C_1N^+$–TSM–pyrene intercalation compounds are shown in Fig. 12. The ratio of monomer to excimer intensity for the $2C_{18}2C_1N^+$–TSM system is two times higher than that for the $C_{18}3C_1N^+$–TSM system, suggesting that the adsorbed pyrene molecules are isolated in the interlayer space of the $2C_{18}2C_1N^+$–TSM compared with those doped in the $C_{18}3C_1N^+$–TSM.

In order to elucidate the difference in the adsorption states, saponite with the C.E.C. of 71 mequiv/100 g clay was used as host material.[71] Because of the lower layer charge density of the saponite compared with that of the montmorillonite, the $2C_{18}2C_1N^+$–saponite showed the smaller basal spacing of 2.2 nm. Judging from the value, the intercalated $2C_{18}2C_1N^+$ ions arranged as a *pseudo*-trimolecular layer in the interlayer space of the saponite similar to that for the $C_{18}3C_1N^+$–montmorillonite. Pyrene was intercalated into the interlayer space of the $2C_{18}2C_1N^+$-saponite and the change inthe fluorescence spectra as a function of the loaded amount was similar

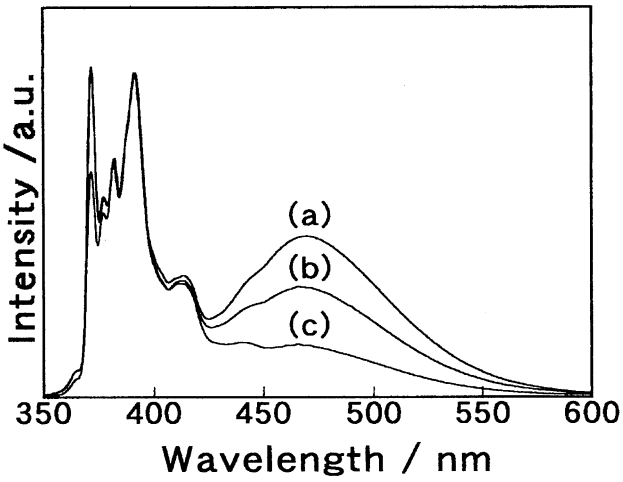

Fig. 12. The emission spectra of (a) the $2C_{18}2C_1N^+$–saponite –pyrene, (b) the $C_{18}3C_1N^+$–TSM– pyrene, and (c) the $2C_{18}2C_1N^+$–TSM–pyrene intercalation compounds. Reprinted from Ref. 71. Copyright 1993 American Chemical Society.

to that observed for the $C_{18}3C_1N^+$–montmorillonite system. The fluorescence spectrum (Fig. 12) showed the tendency of pyrene molecules to form excimer (or dimer) similar to those for the $C_{18}3C_1N^+$–montmorillonite and TSM systems.

These observations indicate that the arrangements of the intercalated alkylammonium ions is the important factor for the difference in the adsorption states of the guest species. When the interlayer alkylammonium ions arranged with the alkyl chain parallel to the silicate sheets, the intercalated pyrene molecules tend to aggregate. On the other hand, the pyrene molecules dispersed effectively when the interlayer alkylammonium ions took a so-called "paraffin type" arrangements. In other words, we can create various reaction environments by selecting the hosts with various layer

charge densities and guests with different size.

It should be noted here that the variation of the *d* values for the $2C_n2C_1N^+$-smectites reported previously.[53—55,70] The difference in the basal spacings corresponds to the difference in the orientation of the alkyl chains. It has been known that excess amount of guest species can be penetrated in the interlayer spaces of smectites as a salt and this phenomena referred as "intersalation". The large *d* values reported in the literatures may be due to the intersalation as well as the difference in the surface layer charge density. Although the difference did not cause the change in the phase transition temperatures, the "intersalation" might affect the photoprocesses of the guest species.

Nakamura and Thomas studied a stable aqueous suspension of hexadecyltrimethylammonium chloride-($C_{16}3C_1NCl$)/laponite system using pyrene as a probe.[72] The suspension contained 2 mmol of $C_{16}3C_1NCl$ and 1 g of laponite (the amount of $C_{16}3C_1NCl$ is two times as much as the cation exchange capacity of laponite). It should be noted that the suspension was able to dissolve 0.1 mmol pyrene. The kinetics of pyrene quenching and pyrene excimer formation reactions suggests that the $C_{16}3C_1NCl$ forms a cluster-like double layer on the clay surface. Since the amount of $C_{16}3C_1NCl$ is two times as much as the C.E.C. of laponite in this system, the effects of Cl^- on the photophysics of adsorbed pyrene can not be excluded.

DellaGuardia and Thomas reported the incorporation of 1-dodecanol and pyrene in the interlamellar space of montmorillonite, which has been revealed from the fluorescence of pyrene and the basal spacing of the compound (interlayer spacing of 13 Å).[73] Upon suspension of the powders in water, a fraction of 1-dodecanol and pyrene are released into the aqueous phase, forming dodecanol micelles into which released pyrene is solubilized.

Photochemical isomerization of *p*-aminoazobenzene intercalated in the hydrophobic interlayer space of alkylammonium–montmorillonite and TSMs has also been investigated.[62—64] Photochromism of azobenzene and its derivatives due to *cis–trans* isomerization has widely been investigated (Scheme 2). Intercalation compounds were obtained by a solid–solid reaction between the organophilic-silicates and *p*-aminoazobenzene and the intercalated *p*-aminoazobenzene showed reversible *trans*-to-*cis* photoisomerization by the UV irradiation and the subsequent thermal treatment (or visible light irradiation). The hydrophobic interlayer spaces of the alkylammonium-silicates were proved to be reaction media for the immobilization and photochemical isomerization of the azo dye.

We have also prepared $2C_n2C_1N^+$–TSM–azobenzene intercalation compounds films by casting the suspension of the $2C_n2C_1N^+$–TSM and azobenzene in organic solvents on a quartz substrate.[64] The intercalated azobenzene exhibits reversible photochromic reactions. The fraction of the photochemically formed *cis*-isomer at the photostationary states depends on the reaction temperature, suggesting the change in the states of the interlayer $2C_n2C_1N^+$. The transition temperatures estimated from the photochemistry of azobenzene were in good agreement with values reported previously.

In order to construct more confined systems where the location and the orientation of the chromophore are controlled precisely, the intercalation of ionic and amphiphilic azo dyes into layered silicates has recently been conducted.[65] The spectroscopic characteristics as well as the photochemistry of the intercalated azo dyes reflected their microstructures which have been controlled by the combination of the molecular structures of the dyes and the type (such as surface layer charge density) of the host lattices.

We have shown that a organically pillared saponite, tetrammethylammonium (TMA)-saponite intercalation compound, can be used as a support to accommodate guest species in the micropore.[74] We have prepared a TMA–saponite–1,4-dihydroxyanthraquinone (abbreviated as DAQ) intercalation compound and investigated its PHB reaction to show the merits of an ordered matrix for a PHB (photochemical hole burning) material. DAQ is one of the molecules most extensively used as a PHB probe and its hole formation has been observed in numerous amorphous matrices so far. It has been suggested that the PHB reaction of DAQ is due to the breakage of internal hydrogen bond(s) and the subsequent formation of external hydrogen bond(s) to proton acceptor(s) in a matrix (Scheme 3).[75] To be a molecularly dispersed system is another basic prerequisite for composing efficient PHB materials to avoid line broadening due to energy transfer. For this purpose, saponite was modified by pillaring with TMA ions to obtain independent micropores in which DAQ molecules were incorporated at a monomolecular level without aggregation. The TMA–saponite can be processed into transparent thin film by casting an aqueous suspension of the TMA–saponite on solid substrate.[20] This ability to

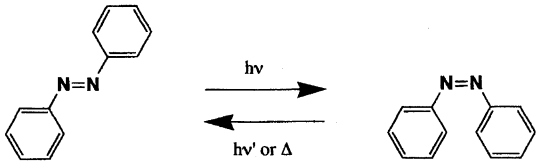

Scheme 2. *cis–trans* isomerization of azobenzene.

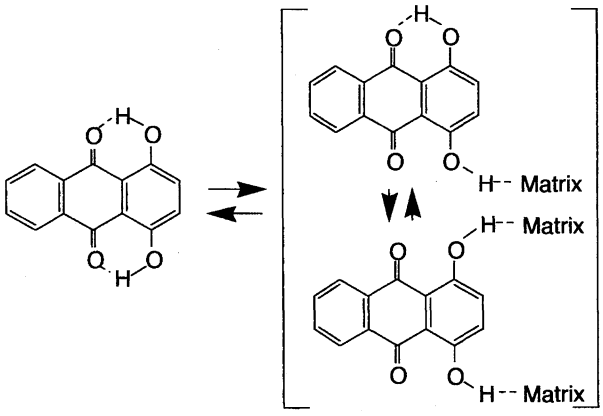

Scheme 3. Photochemical reaction of 1,4-dihydroxyanthraquinone (DAQ).

form films as an assembly of planarly oriented particles is worth noting because other porous materials such as zeolites cannot form oriented thin films by such a simple treatment.

The schematic structure of the TMA–saponite is shown in Fig. 13. The basal spacing of the TMA–saponite was 1.43 nm, indicating that the TMA–pillared interlayer spacing was 0.47 nm. Taking into account the molecular size and shape of DAQ and the geometry of the micropore of TMA–saponite, DAQ was intercalated into the interlayer site of the TMA–saponite with the molecular plane nearly perpendicular to the silicate sheet (Fig. 13).

A persistent spectral zero-phonon hole was obtained at liquid helium temperatures by Kr^+ laser light irradiation (520.8 nm). Figure 14 presents a typical example of the spectra of persistent holes. In spite of the high concentration of DAQ (ca. 1.5 mol kg^{-1}), a narrow hole with the initial width of 0.25 cm^{-1} (4.6 K) was obtained. The observed initial width was apparently narrower, if compared with those (e.g. 0.4—0.8 cm^{-1}) of DAQ doped in ordinary polymers and organic glasses (e.g. PMMA, ethanol/methanol mixed glass) obtained under similar experimental conditions. We consider the associated width to be related mainly to the dephasing but the contribution from the spectral diffusion cannot be neglected. On the other hand, a broad *pseudo*-phonon sidehole, the peak position of which is indicated by an arrow in Fig. 14 and whose shift from the zero-phonon hole is 25 cm^{-1}, seems to appear only after an irradiation larger than 1500 mJ cm^{-2}. In Table 4, hole width, homogeneous width Δw_i, and burning efficiency obtained for 520-nm band are summarized.

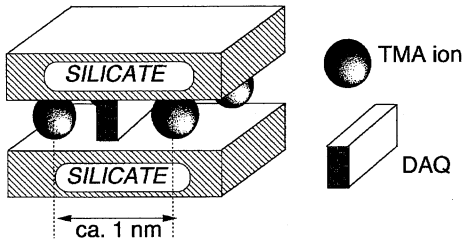

Fig. 13. Schematic drawing for the TMA-saponite-DAQ intercalation compound. Reproduced from Ref. 74. Copyright 1992 American Chemical Society.

The burning efficiency is about 8.3×10^{-4} at the initial stage of burning, estimated from the temporal evolution of the area of zero-phonon hole. This value is almost similar to or seems even higher than the typical one, 1×10^{-4}, observed in ordinary dispersed cases. Taking into account the high concentration of DAQ (ca. 0.15 mol kg^{-1} corresponding to ca. 3 mol dm^{-3}) in the present system, no distinct decreases in the yield also supports the mono-molecular dispersion of DAQ within the interlayer spacing of saponite. This property is most noteworthy from the viewpoint of the fabrication of recording media, because the ability for such high dopant concentration is desirable in preparing materials in thin films. At such high concentrations, the broadening of holes and the decrease in the burning efficiency are usually inevitable in amorphous matrices prepared with conventional procedures.

We assume that the geometry of the microporous structure in the TMA–saponite intercalation compound contributes some desirable characteristics in hole formation though it is still not absolute improvement: relatively narrow zero-phonon hole compared to those in other polar and proton accepting amorphous matrices, performance of high concentration of the PHB centers without decrease of yield, and so on.

We have also developed a technique to prepare a novel inorganic–organic nanocomposite film, TMA–saponite–*p*-nitroaniline (*p*-NA) intercalation compound which showed a optical second harmonic generation.[76] Nonlinear optics comprises the interaction of light with matter to produce a new light field that is different in wavelength or phase.[77] Since nonlinear optical processes provide key functions for pho-

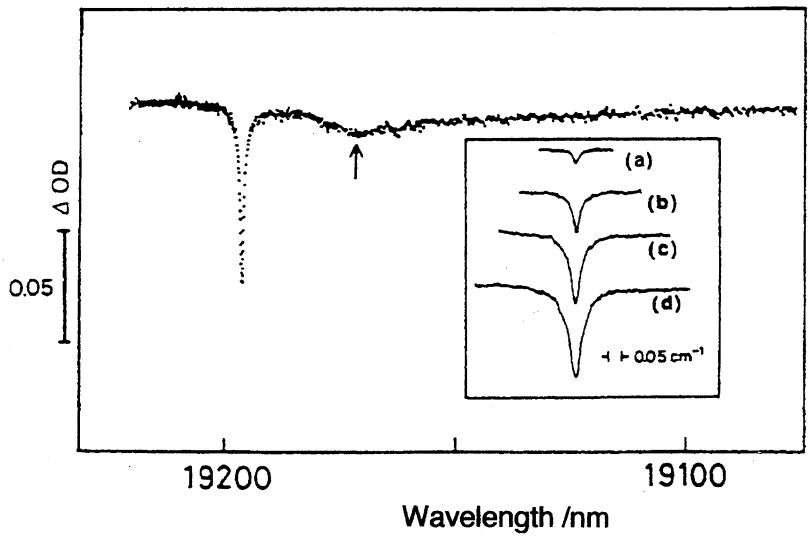

Fig. 14. Zero-phonon hole and *pseudo*-phonon side hole (arrow) burned at 4.6 K by laser light (520.8 nm) irradiation. Insert: Temporal evolution of zero-phonon hole at initial stage of burning. Reprinted from Ref. 74. Copyright 1992 American Chemical Society.

Table 4. Hole Width, Inhomogeneous Width, and Burning Yield Obtained for the 520-nm Band of the TMA–Saponite–DAQ System for Wet and Dried Conditions, Respectively[a)]
Reprinted from Ref. 74. Copyright 1992 American Chemical Society.

Sample	Γ_h/cm^{-1}	$\Delta\omega_i/cm^{-1}$	Φ	λ_B/nm	Comment
Wet	0.25	930	8.3×10^{-4}	520.8	1.3 mJ cm^{-2} 1.4%
Dry	0.38	940	4.5×10^{-4}	520.8	1.3 mJ cm^{-2} 0.5%
Wet	1.38	1040	8.4×10^{-5}	547	1.5 mJ cm^{-2} 0.2%

a) Γ_h: Holewidth, $\Delta\omega_i$: Inhomogeneous width, Φ: Burning yield, λ_B: Burning wavelength, and comment: the laser fluence and relative hole-depth where the parameters are determined. Burning was carried out at 4.6 K.

tonics, recent activity in many laboratories has been directed toward understanding and enhancing second- and third-order nonlinear effects. Second harmonic generation (SHG) is a nonlinear optical process that converts an input optical wave into an outwave of twice the input frequency. Large molecular hyper-polarizabilities β of certain organic materials lead to anomalously large optical nonlinearities. For controlling molecular orientation on a microscopic level, intercalation compounds have potential applicability because intercalated organic species can take unique arrangements in the interlayer space.

The compound was prepared by a solid–gas reaction between a TMA–saponite film and *p*-NA vapor. In order to align *p*-NA dipoles in the TMA–saponite, an external electric field was applied to the host during the intercalation of *p*-NA. The TMA–saponite–*p*-NA intercalation compound prepared under an electric field exhibited SHG, while no SHG was observed for the compound prepared without an electric field. This indicates that the applied electric field caused a noncentrosymmetric alignment of the *p*-NA in the interlayer micropore of the TMA–saponite. The proposed alignment of *p*-NA dipoles in the TMA–saponite is schematically shown in Fig. 15. The TMA–saponite film is composed of oriented particles of TMA–saponite with their *ab* plane parallel to the substrate in which microscopic anisotropy can be directly converted into a macroscopic one. Moreover, the film shows transparency in the visible region and possesses micropore in the interlayer space. Because of the matching between the size and geometry of the micropore of the TMA–saponite and those of *p*-NA molecules, the incorporation into the TMA–saponite is a novel way to create self-assembled aggregates of *p*-NA with noncentrosymmetry.

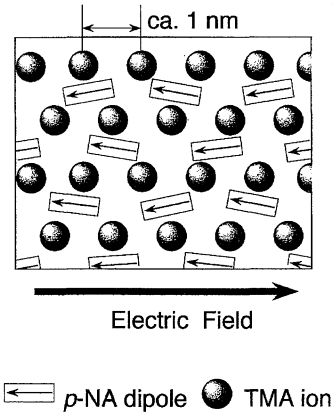

Fig. 15. Schematic structure of the TMA–saponite–*p*-nitroaniline intercalation compounds prepared with an electric field during intercalation. Reprinted from Ref. 76. Copyright 1994 American Chemical Society.

2-5. Photoprocesses of Cationic Photoactive Species Coadsorbed with Organoammonium Ions. Adsorption of cationic dyes on smectites in both the colloidal suspension and in the solid-state has been documented widely. From the change in the absorption spectra, adsorption behavior of the dye molecules has been investigated. The adsorption of cationic dyes such as Methylene Blue,[78)] Pyronine Y,[79)] Rhodamines,[80)] Crystal Violet,[81)] and Cyanine[82)] on smectites has been investigated so far. The concentrations of dyes and hosts, the relative amounts of dye to hosts as well as the nature of the hosts affect the adsorption state of the dyes employed and the differences have been detected by the visible spectroscopy. In some cases, X-ray diffraction data supported the discussion on the adsorption sites and states. The effects of the coadsorption of organoammonium cations on the states of the dye cations have been investigated by means of spectroscopic characteristics.

Cationic pyrene derivatives, (1-pyrenyl)ammoniumtrimethyl (PN^+), [3-(1-pyrenyl)propyl]ammoniumtrimethyl ($P3N^+$), [4-(1-pyrenyl)butyl]ammoniumtrimethyl ($P4N^+$), and [8-(1-pyrenyl)octyl]ammoniumtrimethyl ($P8N^+$) ions have been used to study the anionic surface of silicate sheets.[83—87)] As mentioned earlier on the luminescence of pyrene, Della Guardia and Thomas studied the emission properties of $P4N^+$ adsorbed on colloidal montmorillonite and found that excimers formed even at low concentrations ($1—5\times10^{-6}$ M) of $P4N^+$ (M = mol dm^{-3}).[83)] Figure 16 shows the emission spectra of $P4N^+$ adsorbed on colloidal montmorillonite particles. This indicates a clustering of adsorbed $P4N^+$ on the surface.

Coadsorption of $C_{16}3C_1N^+$ (the amount is 20% of C.E.C.) was carried out by adding an aqueous solution of $C_{16}3C_1N^+$

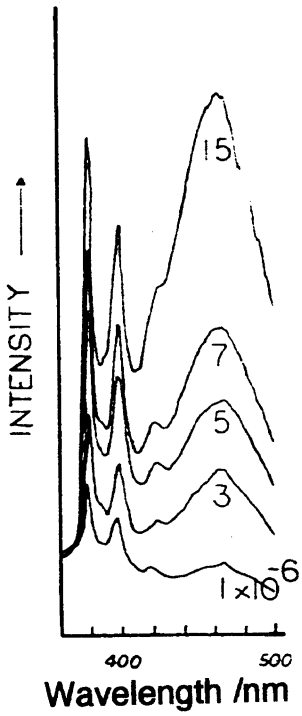

Fig. 16. Fluorescence spectrum of [4-(1-pyrenyl)butyl]trimethylammonium ion ($P4N^+$) adsorbed on colloidal montmorillonite depending on the concentration (1×10^{-6}—1.5×10^{-5} mol dm^{-3}). Reprinted from Ref. 83. Copyright 1983 American Chemical Society.

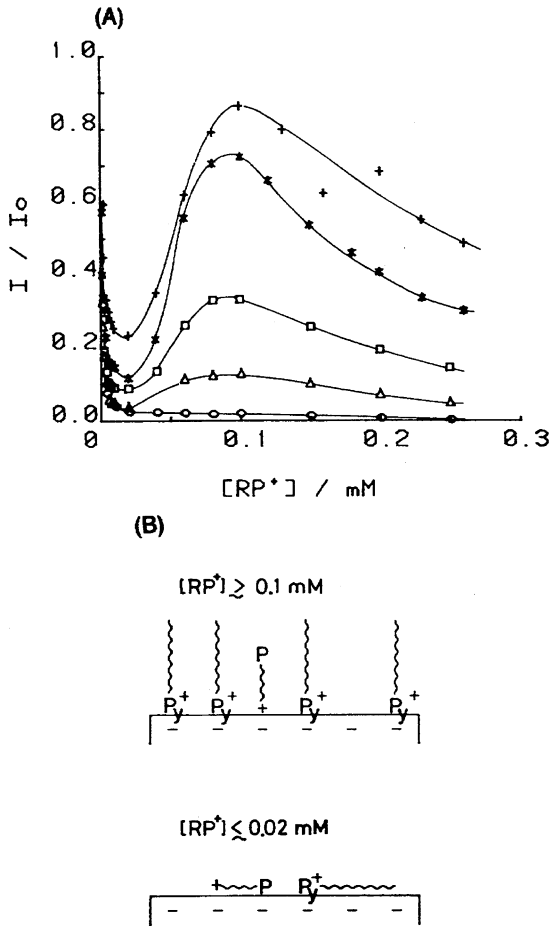

Fig. 17. (A) Influence of the alkyl chain length of various alkylpyridinium ions on the $P4N^+$ fluorescence quenching behaviors in laponite colloids (5g dm^{-3}): (○) ethyl-, (△) pentyl-, (□) octyl-, (×) dodecyl-, (+) hexadecyl-; [$P4N^+$] = 5×10^{-7} M (1 M = 1 mol dm^{-3}). (B) Schematic model for $P4N^+$ fluorescence quenching by alkylpyridinium ions: Py^+, alkylpyridinium ions; + P, $P4N^+$. Reprinted from Ref. 84. Copyright 1987 American Chemical Society.

to the colloidal montmorillonite suspension containing $P4N^+$ (the amount is 0.5 % of C.E.C.).[84] By the addition of $C_{16}3C_1N^+$, the $P4N^+$ can be dispersed over the silicate surface, which causes the emission from the pyrene monomer to increase and the excimer to decrease. Excited state $P4N^+$ exhibited a double-exponential decay, suggesting that there exist two different regions of the particles though the origin is unclear. The quenching study demonstrated that the surfactants reduced the accessibility of quenchers not adsorbed by the clay to the montmorillonite. When quenchers are adsorbed on the montmorillonite, the quenching rate constant is reduced by at least 1 order of magnitude compared to a homogeneous solution.

The fluorescence quenching of $P4N^+$ adsorbed on colloidal laponite by coadsorbed C_nPy^+ ion showed unusual behavior. Figure 17 shows the influence of the alkyl-chain length of various C_nPy^+ ions on the $P4N^+$ fluorescence.[84] Increasing the quencher concentration led to an efficient quenching of $P4N^+$ fluorescence, but increasing the quencher concentration further produced a reverse effect, whereby the fluorescence started to recover, only to be followed by a smaller degree of quenching. The alkyl chain length of the C_nPy^+ ions affects the degree of the recovery. From these observations, a schematic model for PN^+ fluorescence quenching by C_nPy^+ ions is proposed. Thus, it has been revealed that the geometries or arrangements of reactants affect the quenching of the excited adsorbed chromophore on colloidal clay.

Viane et al. studied the adsorption of $P3N^+$ bromide on hectorite, barasym, and laponite by an ion exchange mechanism.[85,86] Even at very low concentrations, a 480-nm emission was observed due to ground state interactions of the adsorbed $P3N^+$ ions, resulting in efficient excimer formation. This indicated a clustering of the adsorbed $P3N^+$ on the silicate surface. The 480-nm emission was suppressed by detergent molecules or Ca^{2+} ions. In the former case, detergent molecules solubilized $P3N^+$ on the surface of laponite as observed in the $P4N^+$-montmorillonite system. On the other hand, the mobility of $P3N^+$ was restricted in the latter case because of the ordering of silicate particles in suspension. Nonhomogeneous distribution of $P3N^+$ ions and a minimization of the contact surface between hydrophobic pyrene derivatives and the surrounding water phase were proposed to explain the excimer formation.

In order to see which was the major determining factor, suspensions in different solvents were studied in their subsequent work.[86] In that study, they used three pyrene derivatives, PN^+, $P3N^+$, and $P8N^+$ bromides. In nonaqueous

suspension, no excimer emission was observed. Since the efficient intermolecular excimer formation in aqueous suspension had been ascribed to a cluster formation, the absence of excimer emission indicated the absence of clusters on the clay surface when the clays were suspended in nonaqueous media. These observations suggested that the distribution of the adsorbed ions is determined by the surrounding medium and not by the distribution of negative adsorption sites and that the bonding between the positive probe and negative site on the clay surface is not strong enough to inhibit diffusion of the adsorbed ions on the clay surfaces.

The adsorption of (9-anthracenemethyl)ammonium ions (abbreviated as AMAC) and P4N$^+$ to a zirconium(IV) phosphate in the presence of butylamine hydrochloride and their binding behavior has been studied.[88,89] AMAC tends to aggregate at the surface of zirconium(IV) phosphate, while P4N$^+$ gives monomer emission when adsorbed on ZrP at low surface coverage. The excimer formation of P4N$^+$ on zirconium(IV) phosphate depends upon the concentration of the phosphate, additives as well as probe. However, the origin of the difference in the binding behavior between AMAC and P4N$^+$ has not been clarified.

Takagi et al. reported the intercalation of 1′,3′,3′-trimethylspiro[2*H*-1-benzopyran-2,2′-indoline] (H-SP) and its 6-nitro (NO_2-SP) and 6-nitro-8-(1-pyridiniomethyl) (Py$^+$-SP) derivatives into montmorillonite, and photochromic behavior has been studied for colloidal systems.[61] The effects of the intercalation on the rate of thermal coloration and decoloration have been compared with those in other systems such as colloidal silica, hexadecyltrimethylammonium bromide, and sodium dodecyl sulphate (SDS) micelles.

Py$^+$-SP was intercalated into montmorillonite quantitatively as an equilibrium mixture with the corresponding MC with the ratio of Py$^+$-Sp : Py$^+$-MC of 35 : 65 and exhibited reversed photochromism. It is known that thermal equilibria between SP and MC are dependent on the polarity of surroundings; MC becomes the major product with increasing polarity. Therefore, the observed reverse photochromism has been explained in terms of the polar interlayer of montmorillonite. The thermal isomerization of Py$^+$-SP intercalated in aqueous colloidal montmorillonite exhibited a linear combination of two components of first order kinetics, indicating the presence of two adsorption environments. It has been suggested that one is due to molecularly separated species and the other is due to aggregated species.

In contrast, a preferential adsorption as SP was observed when $C_{16}3C_1N^+$ was coadsorbed with Py$^+$-SP, H-SP, and NO_2-SP, and normal photochromism has been observed in these systems. Single first-order kinetics has been observed for the Py$^+$-SP–$C_{16}3C_1N^+$–montmorillonite system. The effects of coadsorbing $C_{16}3C_1N^+$ on the photochromic behavior showed that the $C_{16}3C_1N^+$ surrounds Py$^+$-SP to cause hydrophobic surrounding of Py$^+$-SP.

The formation of stable *H* (parallel type) and *J* (head-to-tail type) aggregates of photoinduced merocyanines (PMC) has been suggested in the study on the photochromism of a series of 1′-alkyl-3′,3′-dimethyl-6-nitro-8-(alkanoyloxymethyl)spiro(2*H*-1-benzopyran-2,2′-indoline) derivatives with different length of alkyl chains in $2C_{12}2C_1N^+$–montmorillonite.[60] A cast film consisting of the SP incorporated into a bilayer intercalated into a clay was prepared on a glass plate by slowly evaporating a solution of the SP and $2C_{12}2C_1^+$–montmorillonite. The results of the photochromism of spiropyrans in $2C_{12}2C_1^+$–montmorillonite film are summarized in Table 5. When longer R^1 alkyl chains were introduced, new very sharp absorption peaks at around 500 nm appeared in addition to the absorption at 570 nm due to the monomeric PMC upon UV light irradiation. A new sharp absorption band appeared at a longer wavelength region around 610 nm when SPs bearing longer alkyl chains were exposed to UV light. These new absorption bands are ascribable to aggregates of PMCs which are reported to form occasionally in organized molecular assemblies. The absorption bands around 500 and 610 nm have been ascribed to

Table 5. Photochromism of Spiropyrans (SPs) in $2C_{12}2C_1N^+$–Montmorillonite Cast Film
Reprinted from Ref. 60. Copyright 1990 Royal Society of Chemistry.

			$2C_{12}2C_1N^+$–montmorillonite			λ_{max}/nm[b]	
SP	R^1	R^2	λ_{max}/nm[b]	10^4k/s^{-1} [c]	T/°C	EtOH	*n*-C_6H_{14}
0100	Me	H	552	1.21	37	540	580
1800	$(CH_2)_{17}Me$	H	574	19.3	37	542	576
0112	Me	$CH_2OCOC_{11}H_{23}$	550	2.90	37	542	620
1012	$(CH_2)_9Me$	$CH_2OCOC_{11}H_{23}$	580	11.2	37	547	576
1612	$(CH_2)_{15}Me$	$CH_2OCOC_{11}H_{23}$	493(H), 570	17.5,25.9	60	547	577
1812	$(CH_2)_{17}Me$	$CH_2OCOC_{11}H_{23}$	497(H), 570	16.7,25.0	65	549	580
0822	$(CH_2)_7Me$	$CH_2OCOC_{21}H_{43}$	578	12.7	37	546	578
1822	$(CH_2)_{17}Me$	$CH_2OCOC_{21}H_{43}$	615(J), 566	16.0,16.5	70	553	579
0130	Me	$CH_2OCOC_{29}H_{59}$	565	1.50	37	543	576
1230	$(CH_2)_{11}Me$	$CH_2OCOC_{29}H_{59}$	576	4.58	37	548	577
1830	$(CH_2)_{17}Me$	$CH_2OCOC_{29}H_{59}$	617(J), 566	5.35,2.35	70	548	578

a) The SP/DDAC–Mont molar ratio is 1/2. b) Absorption maximum of PMC. c) The first-order rate constants for the thermal isomerization of PMC to SP at the indicated temperature.

H and *J* aggregates of PMC, respectively. A high activation energy and highly positive activation entropy for *J* and *H* PMCs, which directly correlate with the thermal stability of these aggregates (slow decoloration), have been observed.

The adsorption of N-alkylated Acridine Orange cation on a colloidally dispersed montmorillonite[90] and zirconium-(IV) phosphate[91] has been investigated. The effects of alkyl chain length on the spectroscopic properties revealed that the orientation and mobility of the adsorbed Acridine Oranges changed depending on the alkyl-chain length. The steric hindrance and hydrophobic interaction among the alkyl chains of adjacent dyes are thought to be concerned.

The interlayer spaces of clay minerals have been shown to provide a stable and characteristic reaction field suitable for spatially controlled photochemical reactions. Regioselective photocycloadditions of stilbazolium cations, intercalated in the interlayer space of saponite, has been reported.[92—95] There are four possible reaction paths of the photochemical reactions of the stilbazolium ion (Fig. 18). Upon irradiation of UV light to the suspension of the stilbazolium–saponite system, *syn*-head-to-tail dimers were predominantly formed at the expense of *cis–trans* isomerization which is a major path in a homogeneous solution. The selective formation of head-to-tail dimers suggests that the intercalation occurs in an anti-parallel fashion, as is shown in Fig. 19. Since the dimer yields were barely dependent on the loading amount of the guest ions, stilbazolium ions were adsorbed inhomogeneously to form aggregates with antiparallel alternative orientation even at very low loading (e.g. 1% of C.E.C.) This aggregation was supported by the fluorescence spectrum of the dye adsorbed on saponite, in which excimer fluorescence was observed at 490—515 nm at the expense of the monomer fluorescence at ca. 385—450 nm (Fig. 20). The selective formation of *syn* head-to-tail dimers indicates the formation of aggregates owing to hydrophobic interaction between the adsorbate ions.

The change in the aggregation state of a stilbazolium ion, γ-stilbazolium (4-stirylpyridinium) ion, on saponite by coadsorption of alkylammonium ions (C_nN^+) has been investigated.[95] Figure 21 shows the effect of C_nN^+ on photoreactivity of pre-intercalated stilbazolium ions on clay. On coadsorbing C_8N^+, the major photoreaction was changed from cyclodimerization to *E–Z* isomerization and the excimer emission of the intercalated stilbazolium ions was dramatically reduced. The formation of dimer or cluster of adsorbent is adequately simulated by a Monte Carlo method for a two-dimensional lattice site model.

Photochemical cycloaddition for several unsaturated carboxylates has been studied in the presence of hydrotalcite.[96] Similar to those observed for the effects of the addition of organoammonium ions on the photochemistry of stilbazolium ions on smectite, the addition of sodium *p*-phenethylbenzoate, a photochemically inactive coadsorbate, affected significantly the product distribution in the photolysis of the *p*-styrylbenzoate intercalated in hydrotalcite. This series of investigations shows that the organization of organic species into the interlayer space of layered materials is a way of crystal engineering in which controlled reactions can be obtained. In other words, the discussion based on the selectivity of the reactions and the interlayer spacing is a method of probing the geometric relationships between intercalated species.

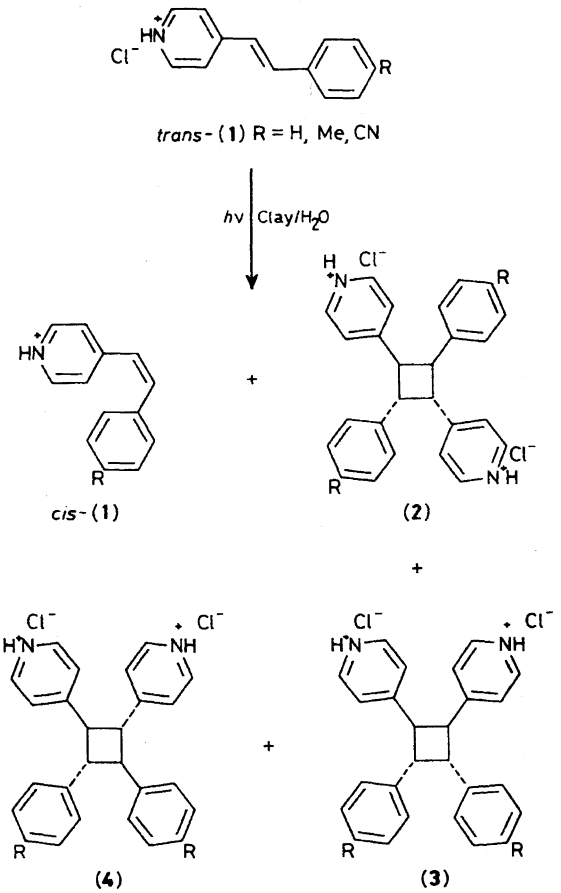

Fig. 18. Four possible reaction paths of the photochemical reactions of the stilbazolium cation. Reproduced from Ref. 92. Copyright 1989 The Royal Society of Chemistry.

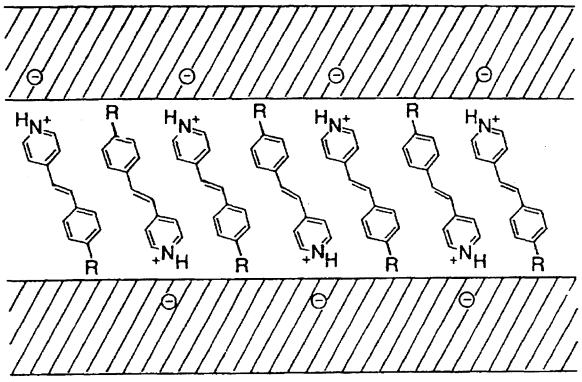

Fig. 19. A schematic representation of the alkene packing in the interlayer space of saponite. Reprinted from Ref. 92. Copyright 1989 The Royal Society of Chemistry.

The aggregations of cationic species has also been controlled by the cointercalation of water soluble polymers. We have prepared the tris(bipyridine)ruthenium(II) fluortetrasilicic mica (TSM)–poly(*N*-vinyl-2-pyrrolidone) (PVP) intercalation compounds with variable concentration of [Ru-

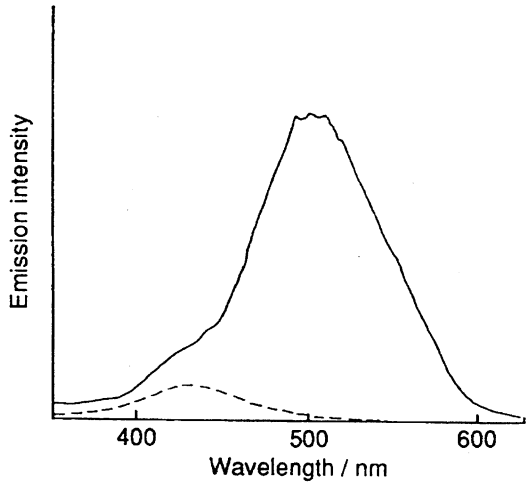

Fig. 20. Emission spectrum of a stilbazolium cation adsorbed on saponite (solid line) and without saponite (broken line). Excited at 330 nm. Reprinted from Ref. 93. Copyright 1990 The Royal Society of Chemistry.

$(bpy)_3]^{2+}$ by cation exchange of sodium ions in the preformed TSM–PVP intercalation compound with $[Ru(bpy)_3]^{2+}$.[97] PVP was added in order to avoid aggregation of $[Ru(bpy)_3]^{2+}$.

The compounds showed unique photoluminescence properties. The luminescence maxima of intercalated $[Ru(bpy)_3]^{2+}$ shifted gradually toward blue with the decrease in the loading of $[Ru(bpy)_3]^{2+}$, reflecting the change in the polarity and/or rigidity of the microenvironment of $[Ru(bpy)_3]^{2+}$, which was caused by cointercalated polar PVP. Moreover, $[Ru(bpy)_3]^{2+}$ was isolated effectively to suppress self quenching even at its high concentration loading. It was supposed that cointercalated PVP was forced to surround $[Ru(bpy)_3]^{2+}$ in close contact in the sterically limited interlayer spaces. The schematic structures are shown in Fig. 22. X-Ray diffraction studies supported the conclusion. When the $[Ru(bpy)_3]^{2+}$ intercalated in the TSM without PVP, the diffraction peaks split into two, suggesting segregation.

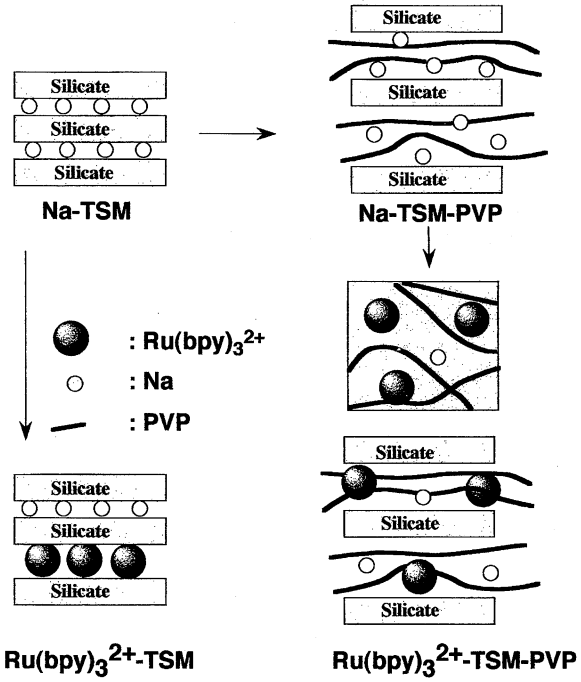

Fig. 22. Schematic structure of (a, top left) Na–TSM, (b, bottom left) Ru(II)–TSM intercalation compound, (c, top right) TSM-PVP intercalation compound, and (d, bottom right) Ru(II)–TSM–PVP intercalation compound. Reprinted from Ref. 97. Copyright 1993 American Chemical Society.

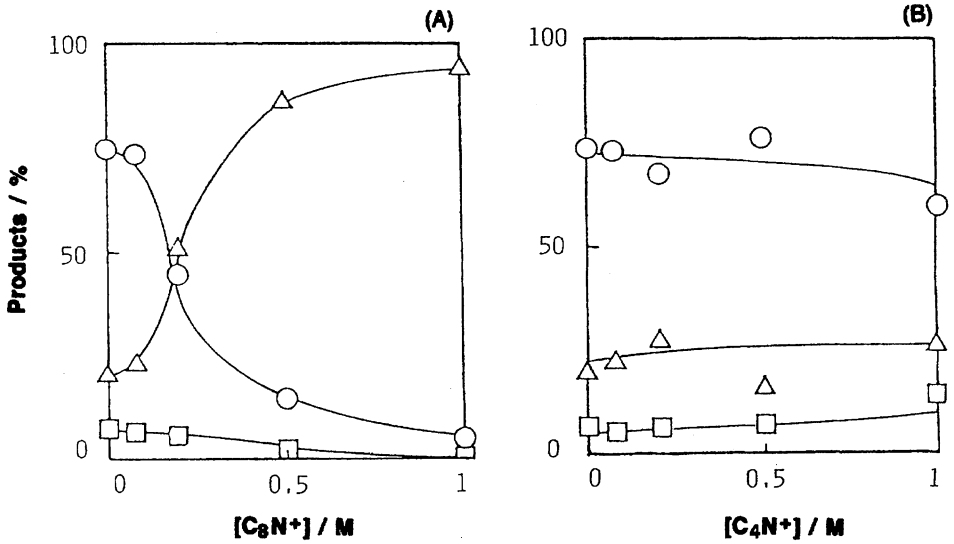

Fig. 21. Effect of alkylammonium ions on photoactivity of pre-intercalated γ-stilbazolium ion on saponite: (-○-), *syn* head-to-tail dimer; (-□-), *syn* head-to-head dimer (**3**); (-△-), *Z*-isomer. Intercalated γ-stilbazolium–saponite complex was suspended in 5 ml of aqueous solution of alkylammonium ions; (A) octylammonium (C_8N^+); (B) butylammonium (C_4N^+). Reprinted from Ref. 95. Copyright 1991 The Chemical Society of Japan.

3. Surfactant Intercalated Silicates as Intermediates for the Surface Modification

3-1. Silylating Reactions of the Interlayer Silanol Groups of Layered Polysilicates. Layered polysilicates such as magadiite and kenyaite are known to form intercalation compounds by cation exchange and adsorption of polar molecules.[98] Since the reactive silanol groups exist in the interlayer surface of these layered silicates, the surface modifications through silylating reactions of the interlayer silanol groups has been investigated.[99—103] The functional unit has been attached to silicate sheet through covalent bond, so that they may exhibit unique adsorptive properties if compared with the organically modified silicates prepared by the ion exchange reactions.

The grafting reaction of interlayer Si–OH groups of magadiite with chlorotrimethylsilane has successfully been achieved by Ruiz-Hitzky and Rojo.[99a] For the reaction to occur, the silicic acid has been expanded by the intercalation of appropriate organic polar molecules such as dimethyl sulfoxide. However, bulky silylating agents could not be intercalated by this method. In order to overcome this limitation, the organoammonium exchanged silicates have been used as intermediates.[100,102] The intercalation of alkyltrimethylammonium ($C_n3C_1N^+$) ions into layered polysilicates has been examined so far. The ion exchange reactions of magadiite, kenyaite, and ilerite with $C_n3C_1N^+$ ions result in the formation of intercalation compounds with expansion of the basal spacings. It seemed that the large interlayer separation by the introduction of the organoammonium ions makes the interlayer Si–OH groups accessible to silylation. Trimethylsilyl derivatives of magadiite, kenyaite, and ilerite have been prepared by this method.[100,102] The X-ray diffraction patterns of the products exhibit the change in the basal spacings. The infrared spectra and nuclear magnetic resonance of the products indicated the existence of the trimethylsilyl group. All these results revealed that the surface silanol groups reacted with trimethylsilyl group to form trimethylsilyl derivatives of the layered silicates. These organic derivatives of layered polysilicates may exhibit unique adsorptive properties being different from those of the silicates with interlayer organoammonium ions, because the organic moiety is attached on the silicate surface with covalent bond. The surface properties of the trimethylsilyl-magadiite, kenyaite, and ilerite have been investigated by nitrogen adsorption/desorption isotherms. The silylated solids showed type I isotherm indicating the microporous structures and the BET surface area is relatively high.

The silylating reaction of chloro(methyl)diphenylsilane with the surface silanol group of magadiite and kenyaite was also conducted.[101] By using the dodecyltrimethylammonium-silicates, it became possible to obtain a methyldiphenylsilyl derivative of magadiite. The large interlayer spacings (the basal spacings of the $C_{12}3C_1N^+$-magadiite and kenyaite wee 2.94 and 3.56 nm, respectively) as well as the hydrophobic nature of the surface of the $C_{12}3C_1N^+$ derivatives led the success in introducing the diphenylmethylsilyl groups. The surface modification of magadiite with various silylating reagents has been conducted using the $C_{12}3C_1N^+$ derivative as the intermediate.[103]

3-2. Guest Displacement. Although the cation exchanges of smectites has been achieved easily in suspension even in the solid-states, some ion exchange reactions do not take place in other layered materials. For the ion exchange of those cations, which do not intercalate directly with the interlayer exchangeable cations, organoammonium-exchanged forms have been used as intermediates. Examples have been seen for the ion exchange with layered titanates, niobates, and layered polysilicates.

Miyata et al. reported the ion exchange of methylviolgen dications (1,1′-dimethyl-4,4′-bipyridinium ion; abbreviated as MV^{2+}) with propylammonium cations which have been pre-intercalated in the interlayer space of tetratitanic acid ($H_2Ti_4O_9$).[104] They have also investigated the photoinduced electron transfer between host lattice and methylviologen. The intercalation of methylviologen into the interlayer spaces of a titanoniobate ($HTiNbO_5$),[105] and the intercalations of methylene blue[106] and 5,10,15,20-tetrakis(1-methyl-4-pyridinio)porphyrin[107] into layered tetratitanic acid have also been achieved by means of the guest exchange method using propylammonium-exchanged materials as intermediates. The guest exchange method has been applied to introduce cationic photoactive species such as tris(bipyridine)-ruthenium(II) cation[108] and *pseudo* isocyanine[109] into magadiite ($Na_2Si_{14}O_{29}\cdot nH_2O$). These successes in introducing guest species by the guest replacement method provide a new opportunity to design functional supramolecular assembly from the organization of guest species into layered solids.

The photochromic behavior of the MV^{2+} intercalated into a series of layered transition metal oxides has been reported.[110] The photochemical studies were conducted for powdered sample by irradiation with Hg lamp and the reaction was monitored by diffuse reflectance spectra. Semiconducting host layers acted as an electron donor for the reduction of viologen to form radical cations of the intercalated MV^{2+} in the interlayer space. The stability of the photochemically formed blue radical cations has been discussed on the basis of their microscopic structures.

It should be noted that the photochemistry of intercalation compounds formed between the layered niobates, $K_4Nb_6O_{17}$ and HNb_3O_8 with MV^{2+} can be controlled by changing the interlayer structures.[110] Two types of MV^{2+} intercalated compounds with different structures have been prepared for each host. In the $K_4Nb_6O_{17}$ system, two intercalation compounds were obtained by changing the reaction conditions. In both of the intercalation compounds, MV^{2+} are located only in interlayer I. HNb_3O_8 also gave two different intercalation compounds; one was prepared by the direct reaction of HNb_3O_8 with MV^{2+} and the other was obtained by using propylammonium-exchanged HNb_3O_8 as an intermediate. In the latter compound, propylammonium ions and MV^{2+} were located in the same layer. The schematic structures are shown in Fig. 23. All the intercalation compounds formed $MV^{\bullet+}$ in the interlayers by host-guest electron transfer. Table 6 shows

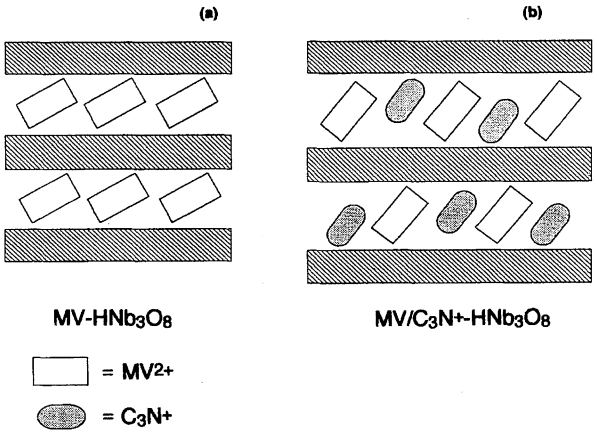

Fig. 23. Schematic representation of the interlayer structure of (a) MV–HNb_3O_8 and (b) MV/C_3N^+–HNb_3O_8. Reprinted from Ref. 110. Copyright 1992 American Chemical Society.

Table 6. Half-Lives of $MV^{\bullet+}$ in Various Intercalation Compounds
Reprinted from Ref. 110. Copyright 1994 American Chemical Society.

	in Oxygen	in Air	in Argon
MV–$K_2Nb_6O_{17}$	15 min	45 min	2 h
MV/K–$K_2Nb_6O_{17}$	2 h	6 h	
MV–HNb_3O_8	3 min	4 min	10 min
MV/PA–HNb_3O_8	1 h	4 h	
MV^{2+}–H_xTiNbO_5	3 min	4 min	20 min

the half-lives of $MV^{\bullet+}$ in the intercalation compounds. The presence of co-intercalated species, K^+ and propylammonium ion in the $K_4Nb_6O_{17}$ and HNb_3O_8 systems, respectively, significantly affected the decay of $MV^{\bullet+}$. This difference was explained by guest–guest interactions which varied with the co-intercalation of photoinactive guests (K^+ and propylammonium ion).

Nakato et al. have extensively investigated the intercalation of $[Ru(bpy)_3]^{2+}$ into the interlayer space of layered titanate and niobates ($K_4Nb_6O_{17}$, $HTiNbO_5$, and $H_2Ti_4O_9$) and found that the microstructure of the resulting intercalation compounds varied depending on the reaction conditions.[111] The reaction conditions include the kind of alkylammonium ions and the reaction period. The guest displacement technique yielded some intercalation compounds where alkylammonium ions were co-intercalated with $[Ru(bpy)_3]^{2+}$ ions, and the cointercalated alkylammonium ions suppressed the self-quenching of adsorbed $[Ru(bpy)_3]^{2+}$ to some extent. The intercalation and the luminescence of $[Ru(bpy)_3]^{2+}$ intercalated in the butylammonium-exchange zirconium(IV) phosphate have also been reported.[112]

Thus, the guest exchange method has been successfully applied to prepare intercalation compounds which are not available by conventional ion exchange methods. Furthermore, the microstructures of the resulting intercalation compounds can be varied by the coexisting photoinactive organoammonium ions.

4. Transformation of Layered Solids into Three Dimensional Porous Solids

A large number of porous aluminosilicates of zeolites have been synthesized since 1950s because they can be used as adsorbents, builders for detergents, catalysts, host materials for nanoscale fabrication, and so on.[113] Porous crystals with novel structures and with various compositions besides aluminosilicates have successfully been synthesized recently. Preparation of porous crystals with large pores has been a major subject among very large number of studies on porous crystals.

4-1. Pillaring of the Layered Structures with Metal Oxides. Pillared layered structure have attracted attention as a new class of porous solids.[114] Metal oxide clusters have been introduced as a pillar to provide micropore in the interlayer space. Smectites have been pillared with various metal oxides and their catalytic and adsorptive properties have been investigated widely. These pillared clays have been prepared by the intercalation of inorganic polycation and the oxidation in the interlayer space or the intercalation of colloidal oxides such as silica. The pillaring procedures developed for smectites are not generally applicable to the wide variety of layered materials which do not spontaneously delaminate in water. Although the pillaring of these layered solids may exhibit unique microstructure and adsorptive and catalytic properties due to the variation in the surface layer charge density, and the surface properties of the host lattices, the preparations of the pillared derivatives have been limited due to the difficulties for the introduction of the pillar.

The successful pillaring has been achieved by using the organoammonium-exchanged forms as intermediates. An organic pillar precursor, such as tetraethyl orthosilicate (TEOS), has been introduced into organophilic interlayer spaces of organoammonium exchanged forms, where it was converted to a metal oxide pillar. This approach has been applied to layered silicates[115–117] as well as to transition metal oxides.[118]

The pillarings of magadiite ($Na_2Si_{14}O_{29}\cdot nH_2O$) and kenyaite ($Na_2Si_{21}O_{43}\cdot nH_2O$) have been reported by the intercalation and polymerization tetraethyl orthosilicate into the octylammonium-intercalated silicates.[115] The calcination of the product in air produces silica-pillared derivatives. The resulting silica-pillared silicates exhibit large BET surface area greater than 500 $m^2\,g^{-1}$.

The octylammonium-octylamine cointercalated magadiite and ilerite ($Na_2Si_8O_{17}\cdot nH_2O$) have also been used as intermediates for the introduction of silica pillar. The resulting silica pillared derivatives showed BET surface area of 500 $m^2\,g^{-1}$ for magadiite and ilerite. The silica pillared ilerite showed the BET surface area of ca. 1100 $m^2\,g^{-1}$ upon calcination at 600 °C and ca. 600 $m^2\,g^{-1}$ even at 900 °C where conventional zeolites tend to collapse. The authors concluded that the silica-pillared ilerite with ca. 1 nm distance between the pillars and 2.6 nm gallery height has the best thermal stability and the highest adsorption volume of all silica-pillared compounds.[116] The formation process has

schematically shown in Fig. 24.

The pillaring procedure has been applied to smectite.[119] The quaternary ammonium cation exchanged fluorohectorite was prepared and allowed to react with the mixture of neutral amine and TEOS for 4 h at ambient temperature. By the calcination at 600 °C, the products have been converted to porous solids with the BET surface areas of 470—750 $m^2 g^{-1}$ with retaining the layered structure which has been evidenced by the X-ray diffractions. The BET surface area as well as their pore size has been adjusted by the choice of the quaternary ammonium ions and neutral amines as shown in Table 7. The mechanism for the formation of the microstructure, where TEOS polymerized to form pillar and the interlayer quaternary ammonium ions form micellar aggregates in the interlayer spaces, has been proposed (Fig. 25).[119b]

The pillaring of layered transition metal oxides has also been achieved by using organoammonium exchanged forms as intermediates.[118] The resulting silica-pillared layered titanates ($K_2Ti_4O_9$ and $Na_2Ti_3O_7$) showed large BET surface area. The surface area and the interlayer spacings for the pillared $Na_2Ti_3O_7$ depend on the size of alkylammonium ion used, suggesting the possibility to control the pore geometry.

The introduction of aluminum polyoxo cations and chromium complex into layered titanates, titanoniobates, niobates, and metal phosphates has been conducted with the aid of the organoammonium modification.[120] By the change in the swelling properties upon the ion exchange

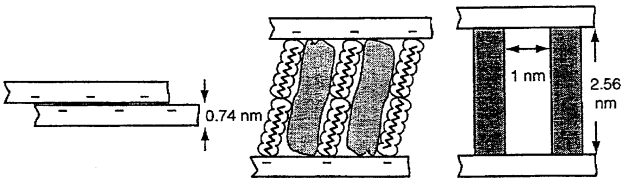

Fig. 24. Schematic drawing for the formation of silica-pillared porous material using the pillaring procedure of H-ilerite with octylamine and TEOS. Reproduced from Ref. 116. Copyright 1995 The Royal Society of Chemistry.

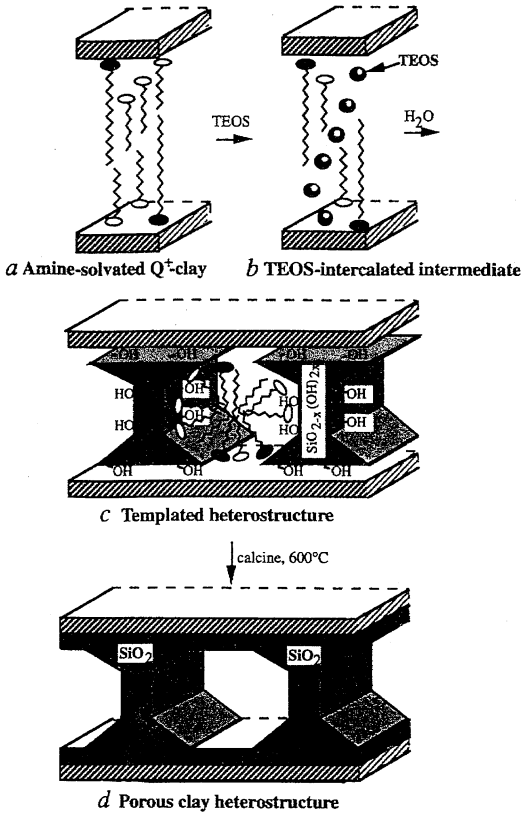

Fig. 25. Proposed mechanism for the formation of a pillared clay heterostructure by gallery templated synthesis. Reprinted from Ref. 119b. Copyright 1995 Nature.

of the interlayer metal ions with organoammonium ion such as tetramethylammonium ions, the introduction of the pillaring species became possible. These pillared-transition metal oxides are promising candidates as a photocatalysts since the host lattices are semiconducting and possess natural quantum well structure.

4-2. Transformation of Kanemite into Mesoporous Silica by the Reaction with Quaternary Ammonium

Table 7. Properties of the Pillared Clay Heterostructures Prepared by Gallery-Templated Synthesis
Reprinted from Ref. 119b. Copy right 1995 Nature.

Alkylammonium exchange ion, Q^-	Amine co-template	PCH[b] pore size / Å	Gallery heights[a]/Å: Clacined PCH	Air-dried heterostructure	Amine-Q^+–FH
$C_{16}H_{33}N(CH_3)_3^+$	$C_6H_{13}NH_2$	15	14.9	22.2	32.2 (30.5)[c]
	$C_8H_{17}NH_2$	17	18.4	22.4	34.4 (33.0)
	$C_{10}H_{21}NH_2$	21	22.4	28.4	36.4 (35.5)
	$C_{12}H_{25}NH_2$	22	23.4	34.4	38.4 (38.0)
$C_{10}H_{21}N(CH_3)_3^+$	$C_{10}H_{21}NH_2$	14	14.3	23.9	29.5 (29.3)

a) Gallery height is defined as the observed X-ray basal spacing minus the 9.6 Å thickness of the clay layer. b) Pore size obtained by Horvath–Kawazoe analysis of N_2 adsorption data. c) Values in parenthesis are the calculated gallery heights for a lipid-like bilayer of Q^+ and neutral amine based on the following estimates of chain lengths (Å): $C_{16}H_{33}N(CH_3)_3^+$, 21.5; $C_{10}H_{21}N(CH_3)_3^+$, 15.3; $C_6H_{13}NH_2$, 9.0; $C_8H_{17}NH_2$, 11.5; $C_{10}H_{21}NH_2$, 14.0; $C_{12}H_{25}NH_2$, 16.5; the observed gallery heights for $C_{16}H_{33}N(CH_3)_3^+$– and $C_{10}H_{21}N(CH_3)_3^+$–FH were 16.5 and 12.4 Å, respectively, as expected for inclined orientations of the chains in the absence of solvating neutral amines.

Ions. Transformation of kanemite ($NaHSi_2O_5 \cdot 3H_2O$ or $NaH[Si_2O_4(OH)_2] \cdot 2H_2O$), a layered polysilicate, to silica-based mesoporous materials has been realized by the reaction with $C_n3C_1N^+$ ions and the subsequent thermal treatment.[121] The pioneering work on kanemite by Lagaly et al.[122] shows various passways to synthesize kanemite and it is routinely prepared by dispersing $Na_2Si_2O_5$ into water. The structure of kanemite is composed of single layered silicate sheets of linked SiO_4 tetrahedra with hydrated sodium ions in the interlayers. When kanemite is allowed to react with $C_n3C_1N^+$ ions, the silicate structure of the product (silicate-organic complexes) shows three-dimensional silica network. Calcination of these materials gives mesoporous silica with narrow pore size distributions and very large surface area (ca. 1000 $m^2\ g^{-1}$). The procedure used is dissimilar to pillaring techniques described above.

Following the disclosure on the formation of mesoporous materials using surfactants, recently developed highly ordered mesoporous materials such as M41S family including hexagonal MCM-41[123] have attracted very diverse attentions. Formed mesopores are ordered and these pores can provide novel nanospaces which can not be supplied by microporous crystals whose micropores are restricted to ca. 1 nm and can not be suitable for the treatment of large molecules. Therefore, the discovery of this group of materials has stimulated many new studies in various research fields.

The interaction of kanemite with $C_n3C_1N^+$ ions was initially investigated by Beneke and Lagaly who reported the formation of intercalation compounds of kanemite with several organoammonium ions.[122] Yanagisawa et al.[121] investigated the reaction of kanemite with several $C_n3C_1N^+$ ions under the same conditions as reported by Beneke and Lagaly. When kanemite was allowed to react with $C_{12}3C_1N^+$ ions, the XRD analysis of the product showed that the peaks due to kanemite almost disappeared and that intense peaks at around *d*-spacings of 3.1 nm and 3.7 nm appeared. The peak of 3.1 nm agreed well with that due to the lamellar phase reported previously.[122] The peak decreased with the reaction time and also disappeared by washing with acetone, supporting that the 3.1 nm phase is lamellar. However, the ^{29}Si NMR result of the reaction product clearly indicated the presence of a Q^4 signal and they concluded that interlayer condensation between adjacent silicate layers occurred. The reactions with other $C_n3C_1N^+$ ions ($n = 14, 16, 18$) also produced similar findings although the *d*-spacings varied according to the chain length.

After the thermal treatment of those silicate-organic complexes at 700 °C, the XRD patterns were similar to those of the as-synthesized materials. It was really a striking feature because layered structure due to silicate-organic systems should normally collapse after the heat treatment at such a high temperature. Therefore, it was reasonable to consider that the three dimensional silica networks were retained after the calcination. The specific surface areas determined by BET method were about 900 $m^2\ g^{-1}$ and, more importantly, the pore size was varied with the chain length of the $C_n3C_1N^+$ ions used (Fig. 26).

Inagaki et al. reported that the formation reaction of silicate-organic complexes used for the preparation of ordered mesoporous silica depended on the degree of ion exchange, expansion of interlayer spacing, and silanol condensation between the layers.[124] By choosing optimum conditions, they obtained highly ordered mesoporous materials with homogeneous mesopores. A typical TEM image of these mesoporous materials is shown in Fig. 27. In those reactions, kanemite was allowed to react with $C_{16}3C_1N^+$ ions at 70 °C for 3 h at relatively high pH values, and then the pH values of the suspension were adjusted at 8.5 to proceed silanol condensation.

The XRD patterns of the as-synthesized and calcined products were characterized as hexagonal, and the specific surface area of the calcined product reached to ca. 1100 $m^2\ g^{-1}$ and the pore size was ca. 2.8 nm. After the reaction with $C_{16}3C_1N^+$ ions, the reaction mixture was separated by centrifugation to remove dissolved silica, thus well resolved XRD pattern of the product has been obtained.

They have proposed folded sheet mechanism of silicate sheets of kanemite with regard to the formation mechanism of

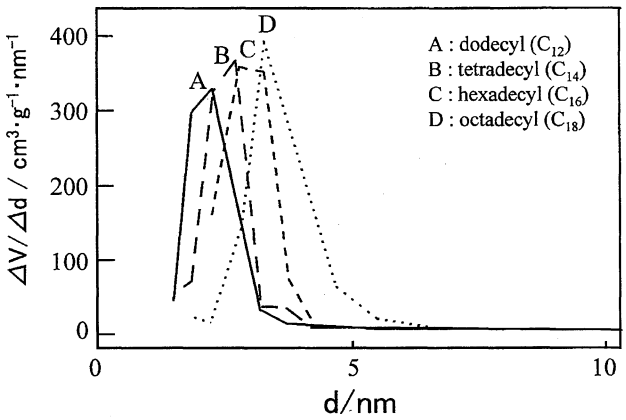

Fig. 26. Pore size distributions of the calcined products derived from the $C_n3C_1N^+$–kanemite complexes after Yanagisawa et al. Reproduced from Ref. 121c. Copyright 1990 The Chemical Society of Japan.

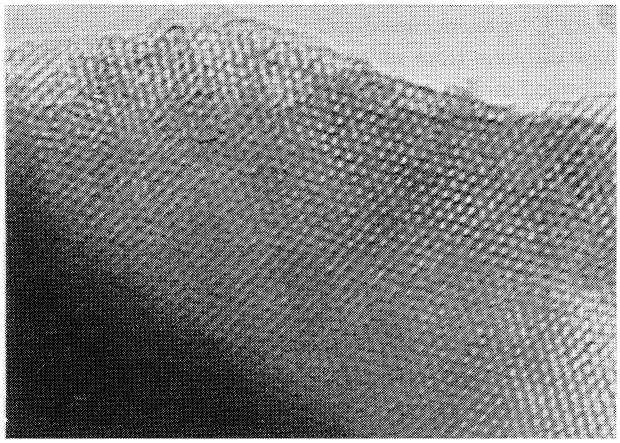

Fig. 27. A typical TEM image of FSM-16.

three dimensional silicate-organic complexes. The proposed formation mechanism involves the intercalation of $C_n3C_1N^+$ ions into the interlayer space of kanemite via the ion-exchange of interlayer sodium ions and subsequent folding and condensation of thin silicate layers. Consequently, the silica-based mesoporous molecular sieves derived from kanemite are called FSM (Folded Sheets Mesoporous Materials). However, this mechanism has not yet been demonstrated, thus further research is necessary for better understanding of the formation mechanism.

Chen and Davis have already reported an extensive study on the difference between MCM-41 and FSM (folded sheet mesoporous materilas).[125] The mesoporous materials derived from kanemite depended on the synthetic conditions used. In some cases, the thermal and hydrothermal stabilities of the materials are higher than those of MCM-41, although both of them showed very similar physicochemical properties. The reason why kanemite derived materials can show higher thermal and hydrothermal stabilities is explained by condensed framework of SiO_2 derived from the layered silicate structure. This difference can be related to the synthetic procedures. In the preparation of MCM-41, the proposed reaction mechanism suggests that silica source should be depolymerized to monosilicic and/or oligo- and poly-silicic acids before organization with surfactants. They have claimed that, in the case of kanemite-derived *meso*-porous materials, the layered structure of kanemite is locally rearranged by the reaction with $C_n3C_1N^+$ ions and that a hexagonal phase formed by condensation of the fragmented layered silicates after their wrapping rodlike micelles, although the conditions employed by Inagaki et al. to form a hexagonal phase are too drastic to retain local environments of the layered nature.

Chen and Davis have also suggested that the reaction conditions are critical for the differentiation between *meso*-porous materials derived from kanemite and MCM-41.[125] They changed the reaction conditions and reported interesting results. They raised the reaction temperature at 80 °C and also changes the amounts of aqueous surfactant solutions to kanemite. In the initial stages of the reactions, they noticed that intercalation compounds formed as reported by Yanagisawa et al.[121] In this early stage, initial condensation of Q^3 sites occurred and it was supposed that lamellar phase different from simple intercalation compounds would be formed in this stage. After the long reaction times, three dimensional silicate network formed and they produced silica-based *meso*-porous materials with high surface area. In any event, there exist some diversity and variation in the structure of MCM-41, depending on the synthetic conditions used by researchers. Thus, future research is truly essential to clarify the difference and nature among these *meso*-porous materials.

Lamellar phases are frequently observed in the case of kanemite. Inagaki et al. reported the formation of lamellar phases by the reaction of kanemite with $2C_n2C_1N^+$ ions or $C_n3C_1N^+$ ions with alcohols.[126] In these cases, the surfactants form lamellar structure, thus inducing the formation of lamellar phases of the silica-surfactant systems. It should be noted that even in these lamellar phases there are some silicon atoms assignable to Q^4 environments, indicating these lamellar phases can not be interpreted as simple intercalation compounds.[126,127] These results should also be related to the formation mechanism of FSM type of *meso*-porous materials.

As described above, depending on the reaction conditions, the characteristics of the products derived from kanemite are different. Variation in the reaction conditions such as pH, surfactant/Si ratio, Na content in kanemite, and so on causes the variation in the structures of the silica-surfactant products. One of the important factors controlling the preparation of the silicate-organic complexes is pH value in the reaction media. The original reports by Lagaly et al.[122] and by Yanagisawa et al.[121] adopted relatively lower pH values around 8.5—9 where the reaction of kanemite with surfactants proceeded for 2 weeks with changing aqueous surfactant solutions once a week. The XRD patterns of the formed silicate-organic complexes only showed a broad peak at around 3.5—4 nm, indicating the formation of disordered *meso*-structured materials.

Based on recent in-situ synchrotron X-ray diffraction data of the formation processes of MCM-41 and FSM type surfactant-contained *meso*-structured materials, the following points can be identified.[128] When kanemite is allowed to react with an $C_n3C_1N^+$ chloride in aqueous solution, a lamellar phase appeared initially. A hexagonal phase appeared after the appearance of lamellar phase. The variation of the patterns is very different from the case of MCM-41 formation where only a hexagonal phase appeared in the early stage of formation of silica-surfactant *meso*-phase formation.

The characteristics of *meso*-porous materials derived from kanemite and MCM-41 have been described in the past of several years. Those results have elucidated that *meso*-porous materials of M41S series and kanemite-derived materials are different in some aspects.

One of the striking characteristics of these materials is their high specific surface areas over 1000 $m^2 g^{-1}$. In a typical N_2 adsorption–desorption isotherm, there is a steep rise at around P/P_0 0.3—0.4. A specific feature is that there is no hysteresis in the region of capillary condensation and this behavior is very characteristic for this class of materials. The pore volume is quite large, reaching almost 1.0 $cm^3 g^{-1}$ in FSM-16.[129]

This silica-based mesoporous materials have unique water adsorption–desorption property.[130] In a typical water adsorption–desorption isotherm of FSM-16, there is a large hysteresis between adsorption and desorption in the range of P/P_0 of 0.3 to 0.8, depending on the pretreatment conditions. This means that these materials can control the medium humidity which is needed to maintain normal environments.

Organic vapors such as benzene and cyclohexane are also adsorbed into these materials very easily even in the very low relative pressures. If compared with the published data on benzene adsorption into MCM-41, the benzene adsorption into FSM-16 is higher and begins at lower relative pressure.

The adsorption volume is quite high than those of zeolites and is possible to be applied for reservoir or recover of waste organic solvents, and so on. Since the *meso*-pores can be used for the precise separation of relatively larger molecules including bioactive substances, it will be very important field in near future.

Surface silanol groups are present in the *meso*-pores, and it is very interesting to modify these silanol groups with various functional groups. We have succeeded in modifying silanol groups with alcohols and silylating reagents.[131] After the modification, surface hydrophobicity and the pore sizes can be tuned. Organometallic complexes have also been fixed in the wall by using MCM-41. Bein et al. have already reported incorporation of conducting polymers into mesopores.[132] The characteristic feature of the *meso*-pores is that the pores are straight channel. It is well known that organization of very minute particles in quantum confinement surroundings exhibits very unique optical and other related properties. Therefore, future studies on optical, electrical, and magnetic properties included in these nanospaces are strongly expected.

Synthesis of mesoporous materials derived from kanemite heavily depends on the synthetic conditions. Characterization on the silicate-organic *meso*-structured materials and their calcined ones as well as the study on the formation processes are one of on-going research themes. These materials provide new possibilities in the fields of catalysts, adsorbents, host matrices for host–guest interactions, and so on. Further studies is essential to clarify the nature of these materials which have potential importance for industrial applications.

5. Conclusions and Future Perspectives

Studies on the applications of organoammonium-exchanged layered solids (mainly silicates) have been reviewed. Surface modifications of swelling layered silicates have been conducted by means of the cation exchange of the interlayer exchangeable cations with organoammonium ions in order to construct supramolecular assembly with specific functions.

The introduction of the organoammonium ions with long chain alkyl groups results in the substantial modification of the hydrophilic surface properties of silicates to strongly organophilic. The organophilic nature of the resulting organoammonium-silicates enabled us to prepare novel supramolecular assembly with hydrophobic guest species in the interlayer spaces. Guest species with photo and catalytic activities have been intercalated in the hydrophobic nanospaces. The dispersion of organically modified silicates in organic polymers to enhance the mechanical properties was a successful example where the silicates can be regarded as a guest in the organic polymers.

A different type of surface modification has been achieved by the ion exchange with small organoammonium ions such as tetramethylammonium ions to produce the microporous structures in the interlayer spaces where the intercalated organoammonium ions act as a pillar. Their confined nanopore has been used for the selective adsorption as well as controlling the states of the adsorbed dyes.

Motivated by the successes in designing materials through the cation exchange of smectites with organoammonium ions, researchers expect novel type of intercalation compounds with specific functions from other layered solids. The combination of the properties and the structures of the hosts and guests may lead novel controlled microstructures.

The conversion of the layered solids to three dimensional nanoporous solids with novel microstructures and adsorptive properties has also been successfully done with the aid of the reactions with organammonium ions.

Precise control of the orientation and distribution of guest species in the two dimensional interlayer spaces of layered solids is very important topics in this research field. The studies on the preparation and the characterization of the intercalation compounds with novel microstructures and the morphology will expand the understanding and advancement of the science and application of the inorganic-organic nanostructured materials.

This work was partially supported by a Grant-in-Aid for Scientific Research, from the Ministry of Education, Science and Culture. Waseda University also supported us financially as a Special Research Project.

References

1) "Comprehensive Supramolecular Chemistry," ed by J. L. Atwood, J. E. D. Davies, D. D. Macnicol, and F. Vögtle, Pergamon, Oxford (1996).

2) a) Special issue on nanostructured materials, *Chem. Mater.*, **8**, (1996); b) D. F. Eaton, in "Advances in the Synthesis and Reactivity of Solids," ed by T. M. Mallouk, JAI Press (1991), Vol. 1, p. 81; c) G. A. Ozin, *Adv. Mater.*, **4**, 612 (1992).

3) "Intercalation Chemistry," ed by M. S. Whittingham and A. J. Jacobson, Academic Press, New York (1982); "Progress in Intercalation Research," ed by W. Müller-Warmuth and R. Schöllhorn, Kluwer Academic Publishers, Dordrecht (1994).

4) a) M. Ogawa and K. Kuroda, *Chem. Rev.*, **95**, 399 (1995); b) R. Schöllhorn, *Chem. Mater.*, **8**, 1747 (1996).

5) G. D. Stucky and J. E. MacDougall, *Science*, **247**, 669 (1990); G. D. Stucky, *Prog. Inorg. Chem.*, **40**, 99 (1992).

6) G. Lagaly and K. Beneke, *Colloid Polym. Sci.*, **269**, 1198 (1991); G. Lagaly, *Solid State Ionics*, **22**, 43 (1986).

7) a) J. H. Clint, "Surfactant Aggregation," Blackie, New York (1992); "Interactions of Surfactants with Polymers and Proteins," ed by E. D. Goddard and K. P. Anathapadmanabhan, CRC Press Inc., Boca Raton (1993); b) H. Ringsdorf, B. Schlarb, and J. Venzmer, *Angew. Chem., Int. Ed. Engl.*, **27**, 113 (1988).

8) a) A. Ulman, "An Introduction to Ultrathin Organic Films," Academic Press, San Diego (1992); b) T. Kunitake, *Angew. Chem., Int. Ed. Engl.*, **39**, 709 (1992).

9) B. K. G. Theng, "The Chemistry of Clay-Organic Reactions," Adam Hilger, London (1974).

10) H. Van Olphen, "An Introduction to Clay Colloid Chemistry," 2nd ed, Wiley-Intersciecnce, New York (1977).

11) M. Ogawa, T. Handa, K. Kuroda, and C. Kato, *Chem. Lett.*, **1990**, 71; M. Ogawa, A. Hagiwara, T. Handa, C. Kato, and K. Kuroda, *J. Porous Mater.*, **1**, 87 (1995).

12) K. Suga and J. F. Rusling, *Langmuir*, **9**, 3649 (1993).

13) R. A. Vaia, R. K. Teukolsky, and E. P. Giannelis, *Chem. Mater.*, **6**, 1017 (1994).
14) G. Lagaly, *Clay Miner.*, **16**, 1 (1981).
15) J. W. Jordan, *J. Phys. Colloid Chem.*, **54**, 294 (1950); K. Khatib, J. Y. Bottero, C. H. Pons, J. P. Uriot, and C. Anselm, *Clay Miner.*, **29**, 401 (1994); T. Permien and G. Lagaly, *Clays Clay Miner.*, **43**, 229 (1995).
16) T. R. Jones, *Clay Miner.*, **18**, 399 (1983).
17) R. M. Barrer, "Zeolites and Clay Minerals as Sorbents and Molecular Sieves," Academic Press, London (1978).
18) R. M. Barrer, *Philos. Trans. R. Soc. London, Ser. A*, **311**, 333 (1984).
19) Y. Kanzaki, M. Kogure, T. Sato, T. Tanaka, and Y. Morikawa, *Langmuir*, **9**, 1930 (1993).
20) M. Ogawa, M. Takahashi, C. Kato, and K. Kuroda, *J. Mater. Chem.*, **4**, 519 (1994).
21) M. Isayama, K. Sakata, and T. Kunitake, *Chem. Lett.*, **1993**, 1283.
22) K. Inukai, Y. Hotta, M. Taniguchi, S. Tomura, and A. Yamagishi, *J. Chem. Soc., Chem. Commun.*, **1994**, 959; Y. Hotta, M. Taniguchi, K. Inukai, and A. Yamagishi, *Clay Miner.*, **32**, 79 (1997).
23) E. R. Kleinfeld and G. S. Ferguson, *Science*, **265**, 370 (1994); E. R. Kleinfeld and G. S. Ferguson, *Chem. Mater.*, **8**, 1575 (1996); Y. Lvov, K. Ariga, I. Ichinose, and T. Kunitake, *Langmuir*, **12**, 3038 (1996); S. W. Keller, H. -N. Kim, and T. E. Mallouk, *J. Am. Chem. Soc.*, **116**, 8817 (1994); T. Sasaki, M. Watanabe, H. Hashizume, H. Yamada, and H. Nakazawa, *Chem. Commun.*, **1996**, 229; T. Sasaki, S. Nakano, S. Yamauchi, and M. Watanabe, *Chem. Mater.*, **9**, 602 (1997).
24) B. K. G. Theng, "Formation and Properties of Clay-Polymer Complexes," Elsevier, Amsterdam (1979).
25) E. Ruitz-Hitzky, *Adv. Mater.*, **5**, 334 (1993).
26) E. P. Giannelis, *Adv. Mater.*, **8**, 29 (1996).
27) Y. Sugahara, N. Yokoyama, K. Kuroda, and C. Kato, *J. Am. Ceram. Soc.*, **67**, C-247 (1984).
28) T. Kyotani, N. Sonobe, and A. Tomita, *Nature*, **331**, 331 (1988); N. Sonobe, T. Kyotani, and A. Tomita, *Carbon*, **26**, 573 (1988); N. Sonobe, T. Kyotani, Y. Hishiyama, M. Shiraishi, and A. Tomita, *J. Phys. Chem.*, **92**, 7029 (1988); N. Sonobe, T. Kyotani, and A. Tomita, *Carbon*, **28**, 483 (1990).
29) Y. Sugahara, Y. Nomizu, K. Kuroda, and C. Kato, *Yogyo-Kyokai-Shi.*, **95**, 134 (1987); Y. Sugahara, K. Sugimoto, T. Yanagisawa, Y. Nomizu, K. Kuroda, and C. Kato, *Yogyo-Kyokai-Shi.*, **95**, 117 (1987).
30) Y. Sugahara, N. Yokoyama, K. Kuroda, and C. Kato, *Ceram. Int.*, **14**, 163 (1988).
31) Y. Fukushima and S. Inagaki, *J. Inclusion Phenom.*, **5**, 473 (1987); Y. Fukushima, A. Okada, M. Kawasumi, T. Kurauchi, and O. Kamigaito, *Clay Miner.*, **23**, 27 (1988); A. Usuki, Y. Kojima, M. Kawasumi, A. Okada, Y. Fukushima, T. Kurauchi, and O. Kamigaito, *J. Mater. Res.*, **8**, 1179 (1993).
32) P. B. Messersmith and E. P. Giannelis, *Chem. Mater.*, **6**, 1719 (1994).
33) T. Lan, P. D. Kaviratna, and T. J. Pinnavaia, *Chem. Mater.*, **6**, 573 (1994).
34) T. Lan and T. J. Pinnavaia, *Chem. Mater.*, **6**, 2216 (1994).
35) T. Lan, P. D. Kaviratna, and T. J. Pinnavaia, *Chem. Mater.*, **7**, 2144 (1995).
36) H. Shi, T. Lan and T. J. Pinnavaia, *Chem. Mater.*, **8**, 1584 (1996).
37) a) R. A. Vaia, H. Ishii, and E. P. Giannelis, *Chem. Mater.*, **5**, 1694 (1993); b) R. A. Vaia, S. Vasudevan, W. Krawiec, L. G. Scanlon, and E. P. Giannelis, *Adv. Mater.*, **7**, 154 (1995).
38) R. A. Vaia, K. D. Jandt, E. J. Kramer, and E. P. Giannelis, *Chem. Mater.*, **8**, 2628 (1996).
39) G. A. Garwood, M. M. Mortland, and T. J. Pinnavaia, *J. Mol. Catal.*, **22**, 153 (1983).
40) S. Boyd and M. M. Mortland, *J. Mol. Catal.*, **34**, 1 (1986).
41) a) M. M. Mortland, S. Shaobai, and S. A. Boyd, *Clays Clay Miner.*, **34**, 581 (1986); b) S. A. Boyd, J. F. Lee, and M. M. Mortland, *Nature*, **333**, 345 (1988); c) S. A. Boyd, S. Shaobai, J. F. Lee, and M. M. Mortland, *Clays Clay Miner.*, **36**, 125 (1988); d) W. F. Jaynes and S. A. Boyd, *Soil Sci. Soc. Am. J.*, **55**, 43 (1991); e) S. A. Boyd, M. M. Mortland, and C. T. Chiou, *Soil Sci. Soc. Am. J.*, **52**, 652 (1988); f) J. A. Smith, P. R. Jaffe, and C. T. Chiou, *Environ. Sci. Technol.*, **24**, 1167 (1990).
42) M. J. Dickey and K. T. Carron, *Langmuir*, **12**, 2226 (1996).
43) J. Bors, A. Gorny, and S. Dultz, *Clay Miner.*, **32**, 21 (1997).
44) a) K. R. Srinivasan and H. S. Fogler, *Clays Clay Miner.*, **38**, 277 (1990); b) K. R. Srinivasan and H. S. Fogler, *Clays Clay Miner.*, **38**, 287 (1990); c) H. Khalaf, O. Bouras, and V. Perrichon, *Microporous Mater.*, **8**, 141 (1997).
45) a) Y. Yan and T. Bein, *Chem. Mater.*, **5**, 905 (1993); b) Y. Yan and T. Bein, *J. Phys. Chem.*, **96**, 9387 (1992).
46) M. Harper and C. J. Purnell, *Environ. Sci. Technol.*, **24**, 55 (1990).
47) R. M. Barrer and G. S. Perry, *J. Chem. Soc.*, **1961**, 850.
48) a) J. F. Lee, M. M. Mortland, and S. A. Boyd, *J. Chem. Soc., Faraday Trans. 1*, **85**, 2953 (1989); b) J. F. Lee, M. M. Mortland, C. T. Chiou, D. E. Kile, and S. A. Boyd, *Clays Clay Miner.*, **38**, 113 (1990).
49) R. K. Kukkadapu and S. A. Boyd, *Clays Clay Miner.*, **43**, 318 (1995).
50) W. F. Jaynes and S. A. Boyd, *Clays Clay Miner.*, **39**, 428 (1991).
51) a) J. J. Stevens and S. J. Anderson, *Clays Clay Miner.*, **44**, 132 (1996); b) J. J. Stevens and S. J. Anderson, *Clays Clay Miner.*, **44**, 142 (1996).
52) a) N. Hu and J. F. Rusling, *Anal. Chem.*, **63**, 2163 (1991); b) J. F. Rusling, M. A. Ahmadai, and N. Hu, *Langmuir*, **8**, 2455 (1992); c) S. Zhang and J. F. Rusling, *Environ. Sci. Technol.*, **29**, 1195 (1995); d) J. F. Rusling, *Acc. Chem. Res.*, **24**, 75 (1991).
53) Y. Okahata and A. Shimizu, *Langmuir*, **5**, 954 (1989).
54) M. F. Ahmadi and J. F. Rusling, *Langmuir*, **11**, 94 (1995).
55) T. Seki and K. Ichimura, *Macromolecules*, **23**, 31 (1990).
56) J. F. Rusling, C. -N. Shi, and S. Suib, *J. Electroanal. Chem.*, **245**, 331 (1988); B. Brahimi, P. Labbe, and G. Reverdy, *J. Electroanal. Chem.*, **267**, 343, (1989); P. Joo, *Colloids Surfaces*, **49**, 29 (1990).
57) "Photochemistry on Solid Surfaces," ed by M. Anpo and T. Matsuura, "Studies in Surface Science and Catalysis 47," Elsevier, Amsterdam (1989); "Surface Photochemistry," ed by M. Anpo, Wiley Interscience, Chichester (1997); "Molecular Dynamics in Restricted Geometries," ed by J. Klafter and J. M. Drake, Wiley Interscience, New York (1989); "23 Photochemistry in Organized & Constrained Media," ed by V. Ramamurthy, VCH Publishers Inc., New York (1991).
58) "Photochromism Molecules and Systems," ed by H. Dürr, and H. Bouas-Laurent, Elsevier, Amsterdam (1990).
59) J. M. Adams and A. J. Gabbutt, *J. Incl. Phenom.*, **9**, 63 (1990).
60) H. Tomioka and T. Itoh, *J. Chem. Soc., Chem. Commun.*, **1991**, 532.

61) K. Takagi, T. Kurematsu, and Y. Sawaki, *J. Chem. Soc., Perkin Trans. 2*, **1991**, 1517.
62) M. Ogawa, K. Fujii, K. Kuroda, and C. Kato, *Mater. Res. Soc. Symp. Proc.*, **233**, 89 (1991).
63) M. Ogawa, H. Kimura, K. Kuroda, and C. Kato, *Clay Sci.*, **10**, 57 (1996).
64) M. Ogawa, M. Hama, and K. Kuroda, manuscript in preparation.
65) M. Ogawa, *Chem. Mater.*, **8**, 1347 (1996).
66) M. Ogawa, M. Yamamoto, and K. Kuroda, manuscript in preparation.
67) H. Miyata, Y. Sugahara, K. Kuroda, and C. Kato, *J. Chem. Soc., Faraday Trans. 1*, **83**, 1851 (1987).
68) A. Nakajima, *Bull. Chem. Soc. Jpn.*, **44**, 3272 (1971).
69) M. Ogawa, H. Shirai, K. Kuroda, and C. Kato, *Clays Clay Miner.*, **40**, 485 (1992).
70) M. Ogawa, T. Aono, K. Kuroda, and C. Kato, *Langmuir*, **9**, 1529 (1993).
71) M. Ogawa, T. Wada, and K. Kuroda, *Langmuir*, **11**, 4598 (1995).
72) T. Nakamura and J. K. Thomas, *Langmuir*, **3**, 234 (1987).
73) R. A. DellaGuardia and J. K. Thomas, *J. Phys. Chem.*, **88**, 964 (1984).
74) M. Ogawa, T. Handa, K. Kuroda, C. Kato, and T. Tani, *J. Phys. Chem.*, **96**, 8116 (1992).
75) "Persistent Spectral Hole Burning: Science and Applications," ed by W. E. Moerner, Springer-Verlag, Berlin (1988).
76) M. Ogawa, M. Takahashi, and K. Kuroda, *Chem. Mater.*, **6**, 715 (1994).
77) a) P. N. Prasad and D. J. Williams, "Introduction to Nolinear Optical Effects in Molecules and Polymers," Wiley Interscience, New York (1991); b) "Principles and Applications of Nonlinear Optical Materials," ed by R. W. Munn and C. N. Ironside, CRC, London (1993).
78) a) P. T. Hang and G. W. Brindley, *Clays Clay Miner.*, **18**, 203 (1970); b) S. Yariv and D. Lurie, *Isr. J. Chem.*, **9**, 537 (1971); c) J. Cenes and R. A. Schoonheydt, *Clays Clay Miner.*, **36**, 214 (1988); d) R. A. Schoonheydt and L. Heughebaert, *Clay Miner.*, **27**, 91 (1992).
79) Z. Grauer, G. L. Grauer, D. Avnir, and S. Yariv, *J. Chem. Soc., Faraday Trans. 1*, **83**, 1685 (1987).
80) a) G. L. Grauer, D. Avnir, and S. Yariv, *Can. J. Chem.*, **62**, 1889 (1984); b) M. J. T. Estévez, F. L. Arbeloa, T. L. Arbeloa, and I. L. Arbeloa, *Langmuir*, **9**, 3629 (1994); T. Endo, N. Nakada, T. Sato, and M. Shimada, *J. Phys. Chem. Solids*, **49**, 1423 (1988).
81) R. Cohen and S. Yariv, *J. Chem. Soc., Faraday Trans. 1*, **80**, 1705 (1984).
82) M. Ogawa, R. Kawai, and K. Kuroda, *J. Phys. Chem.*, **100**, 16218 (1996).
83) R. A. DellaGuardia and J. K. Thomas, *J. Phys. Chem.*, **87**, 3550 (1983).
84) T. Nakamura and J. K. Thomas, *J. Phys. Chem.*, **90**, 641 (1986).
85) K. Viane, J. Caigui, R. A. Schoonheydt, and F. C. De Schryver, *Langmuir*, **3**, 107 (1987).
86) K. Viane, R. A. Schoonheydt, M. Cruzen, B. Kunyima, and F. C. De Schryver, *Langmuir*, **4**, 749 (1988).
87) B. Kunyima, K. Viane, M. M. Hassan Khalil, R. A. Schoonheydt, M. Cruzen, and F. C. De Schryver, *Langmuir*, **6**, 482 (1990).
88) C. V. Kumar, E. H. Asuncion, and G. Roenthal, *Microporous Mater.*, **1**, 123 (1993).
89) C. V. Kumar, E. H. Asuncion, and G. Roenthal, *Microporous Mater.*, **1**, 299 (1993).
90) A. Yamagishi and M. Soma, *J. Phys. Chem.*, **85**, 3090 (1981).
91) M. Taniguchi, A. Yamagishi, and T. Iwamoto, *J. Phys. Chem.*, **94**, 2534 (1990).
92) K. Takagi, H. Usami, H. Fukaya, and Y. Sawaki, *J. Chem. Soc., Chem. Commun.*, **1989**, 1174.
93) H. Usami, K. Takagi, and Y. Sawaki, *J. Chem. Soc., Perkin Trans. 2*, **1990**, 1723.
94) H. Usami, K. Takagi, and Y. Sawaki, *J. Chem. Soc., Faraday Trans.*, **88**, 77 (1992).
95) H. Usami, K. Takagi, and Y. Sawaki, *Bull. Chem. Soc. Jpn.*, **64**, 3395 (1991).
96) a) K. Takagi, T. Shichi, H. Usami, and Y. Sawaki, *J. Am. Chem. Soc.*, **115**, 4339 (1993); b) T. Shichi, K. Takagi, and Y. Sawaki, *Chem. Lett.*, **1996**, 781; c) T. Shichi, K. Takagi, and Y. Sawaki, *Chem. Commun.*, **1996**, 2027.
97) M. Ogawa, M. Inagaki, N. Kodama, K. Kuroda, and C. Kato, *J. Phys. Chem.*, **97**, 3819 (1993).
98) G. Lagaly, *Adv. Colloid Interface Sci.*, **11**, 105 (1979).
99) a) E. Ruiz-Hitzky and M. Rojo, *Nature*, **287**, 28 (1980); b) E. Ruiz-Hitzky, M. Rojo and G. Lagaly, *Colloid Polym. Sci.*, **263**, 1025 (1985).
100) T. Yanagisawa, K. Kuroda, and C. Kato, *React. Solids*, **5**, 167 (1986).
101) T. Yanagisawa, K. Kuroda, and C. Kato, *Bull. Chem. Soc. Jpn.*, **61**, 3743 (1988).
102) K. Endo, Y. Sugahara, and K. Kuroda, *Bull. Chem. Soc. Jpn.*, **67**, 3352 (1994).
103) K. Kuroda et al., manuscript in preparation.
104) H. Mityata, Y. Sugahara, K. Kuroda, and C. Kato, *J. Chem. Soc., Faraday Trans. 1*, **1988**, 2677.
105) T. Nakato and K. Kuroda, *Eur. J. Solid State Chem.*, **32**, 809 (1995).
106) T. Nakato, Y. Iwata, K. Kuroda, and C. Kato, *J. Inclusion Phenom. Mol. Recog.*, **13**, 249 (1992).
107) T. Nakato, Y. Iwata, K. Kuroda, M. Kaneko, and C. Kato, *J. Chem. Soc., Dalton Trans.*, **1993**, 1405.
108) M. Ogawa and N. Maeda, submitted for publication.
109) M. Ogawa, N. Miyamoto, and K. Kuroda, unpublished results.
110) T. Nakato, K. Kuroda, and C. Kato, *Chem. Mater.*, **4**, 128 (1992).
111) a) T. Nakato, D. Sakamoto, K. Kuroda, M. Kaneko, and C. Kato, *Bull. Chem. Soc. Jpn.*, **65**, 322 (1992); b) T. Nakato, K. Kusunoki, K. Yoshizawa, K. Kuroda, and M. Kaneko, *J. Phys. Chem.*, **99**, 17896 (1995).
112) C. V. Kumar and Z. J. Williams, *J. Phys. Chem.*, **99**, 17632 (1995).
113) R. M. Barrer, "Hydrothermal Chemistry of Zeolites," Academic Press, London (1982).
114) "Pillared Layered Structure," ed by I. V. Mitchell, Elsevier, London (1990).
115) J. S. Dailey and T. J. Pinnavaia, *Chem. Mater.*, **4**, 855 (1992).
116) K. Kosuge and A. Tsunashima, *J. Chem. Soc., Chem. Commun.*, **1995**, 2427.
117) S. T. Wong and S. Cheng, *Chem. Mater.*, **5**, 167 (1993).
118) M. E. Landis, B. A. Aufdembrink, P. Chu, I. D. Johnson, G. W. Kirker, and M. K. Rubin, *J. Am. Chem. Soc.*, **113**, 3189 (1991).
119) a) L. J. Michot, O. Barres, E. L. Hegg, and T. J. Pinnavaia, *Langmuir*, **9**, 1794 (1993); b) A. Galarneau, A. Barodawalla, and

T. J. Pinnavaia, *Nature*, **374**, 529 (1995); c) W. L. Ijdo, T. Lee, and T. J. Pinnavaia, *Adv. Mater.*, **8**, 79 (1996).

120) a) W. Hou, Q. Yan, B. Peng, and X. Fu, *J. Mater. Chem.*, **5**, 109 (1995); b) S. Cheng and T.-C. Wang, *Inorg. Chem.*, **28**, 1283 (1989); c) P. Maireles-Torres, P. Olivera-Pastor, E. Rodriguez-Castellon, and A. Limenez-Lopez, *J. Solid State Chem.*, **94**, 368 (1991).

121) a) T. Shimizu, T. Yanagisawa, K. Kuroda, and C. Kato, "Annual Meeting of the Chemical Society of Japan," (1988) Abstract No. 1XII D42 (I-761); b) K. Kuroda, T. Yanagisawa, T. Shimizu, C. Kato, "Abstracts of the 9th Int. Clay Conf. Strasbourg (1989)," p. 222; c) T. Yanagisawa, T. Shimizu, K. Kuroda, and C. Kato, *Bull. Chem. Soc. Jpn.*, **63**, 988 (1990); d) T. Yanagisawa, T. Shimizu, K. Kuroda, and C. Kato, *Bull. Chem. Soc. Jpn.*, **63**, 1535 (1990).

122) K. Beneke and G. Lagaly, *Am. Miner.*, **62**, 763 (1977).

123) a) C. T. Kresge, M. E. Leonowicz, W. J. Roth, J. C. Vartuli, and J. S. Beck, *Nature*, **359**, 710 (1992); b) J. S. Beck, J. C. Vartuli, W. J. Roth, M. E. Leonowicz, C. T. Kresge, K. D. Schmitt, C. T.-W. Chu, D. H. Olson, E. W. Sheppard, S. B. McCullen, J. B. Higgins, and J. L. Schlenker, *J. Am. Chem. Soc.*, **114**, 10834 (1992).

124) a) S. Inagaki, Y. Fukushima, and K. Kuroda, *J. Chem. Soc., Chem. Commun.*, **1993**, 680; b) S. Inagaki, A. Koiwai, N. Suzuki, Y. Fukushima, and K. Kuroda, *Bull. Chem. Soc. Jpn.*, **69**, 1449 (1996); c) Y. Fukushima, S. Inagaki, and K. Kuroda, *Nippon Kagaku Kaishi*, **1995**, 327.

125) C. -Y. Chen and M. E. Davis, *Microporous Mater.*, **4**, 1 (1995).

126) S. Inagaki, Y. Fukushima, and K. Kuroda, *Stud. Surf. Sci. Catal.*, **84**, 125 (1994).

127) N. Okazaki, Y. Sugahara, and K. Kuroda, in preparation.

128) S. O'Brien, R. J. Francis, S. J. Price, D. O'Hare, S. M. Clark, N. Okazaki, and K. Kuroda, *J. Chem. Soc., Chem. Commun.*, **1995**, 2423.

129) P. J. Branton, K. Kaneko, N. Setoyama, K. S. W. Sing, S. Inagaki, and Y. Fukushima, *Langmuir*, **12**, 599 (1996).

130) S. Inagaki, Y. Fukushima, K. Kuroda, and K. Kuroda, *J. Colloid Interface Sci.*, **180**, 623 (1996).

131) S. Saeki, K. Kuroda, Y. Sugahara, and K. Kuroda, in preparation (1996).

132) C. -G. Wu and T. Bein, *Science*, **264**, 1757 (1994).

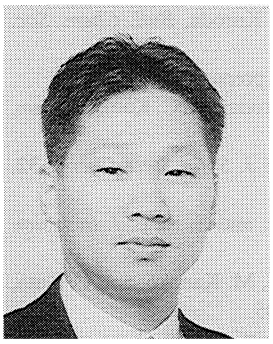

Makoto Ogawa was born in Shizuoka, Japan in 1964. He received his B.S. and M.S. degrees in Applied Chemistry from Waseda University in 1987 and 1989. His doctorate was earned at Waseda University in 1992 under the direction of Professor Chuzo Kato. Then he moved to The Institute of Physical and Chemical Research (RIKEN) as a special researcher for the basic science program, Science and Technology Agency, Japan. He is presently a researcher of PRESTO, Japan Science and Technology Corporation, and assistant professor of the Institute of Earth Science, Waseda University.

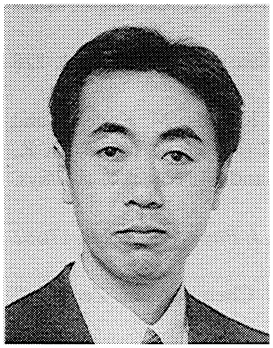

Kazuyuki Kuroda is currently a professor of the Department of Applied Chemistry at Waseda University, where he has been since 1989. He received his doctorate from Waseda University in 1979 under the supervision of Professor Chuzo Kato. His research interests are centered around inorganic materials chemistry and include intercalation chemistry of inorganic layered materials, silicate chemistry, inorganic polymers, inorganic–organic interactions, and functional oxide materials.